NAT. CROAT. | VOL. 35 | No 2 | 0 - 0 | ZAGREB | December 31, 2026

original scientific paper/izvorni znanstveni rad
DOI 10.20302/NC.2026.35.24

FIRST COMPREHENSIVE DESCRIPTION OF THE ENDEMIC CROATIAN POLYTRICHOUS SCORPION *EUSCORPIUS LAGOSTAE* DI CAPORIACCO, 1950 (SCORPIONES, EUSCORPIIDAE)

VALERIO VIGNOLI[1]*, MARTINA PODNAR[2], DEJAN KULIJER[3] & NIKOLA TVRTKOVIĆ[4]

[1]Siena, Italy (e-mail: vignoliv@gmail.com)
[2]Croatian Natural History Museum, Demetrova 1, 10000 Zagreb, Croatia (e-mail: martina.podnar@hpm.hr)
[3]National Museum of Bosnia and Herzegovina, Sarajevo, Bosnia and Herzegovina (e-mail: dejan.kulijer@gmail.com)
[4]Croatian Biospeleological Society, Rooseveltov trg 6, 10000 Zagreb, Croatia (e-mail: nikolatvrtkovic71@gmail.com)

Vignoli, V., Podnar, M., Kulijer, D. & Tvrtković, N.: First comprehensive description of the endemic Croatian polytrichous scorpion *Euscorpius lagostae* Di Caporiacco, 1950 (Scorpiones, Euscorpiidae. Nat. Croat., Vol. 35, No. 2, _____, 2026, Zagreb.

Euscorpius lagostae Di Caporiacco, 1950, a poorly studied endemic species belonging to the *Euscorpius hadzii* Di Caporiacco, 1950 species complex, is redescribed with the first morphological illustrations and confirmed by molecular phylogenetic analysis based on broader sampling. New distribution records of *E. lagostae* from the western part of the Pelješac Peninsula, and Hvar Island are presented, and the first ecological insights into this neglected species are provided. This study represents the first step toward resolving the taxonomic status of the genetically closest taxa distributed along the coastal area from the Neretva River mouth to Montenegro, including the southeastern coast of the Pelješac Peninsula, Lokrum and Mljet Islands, and southern Herzegovina. Newly collected samples near Višegrad in the northeastern Dinarides (Bosnia and Herzegovina) and near the Adriatic coast, close to the Neretva River mouth (Croatia), revealed deeply divergent genetic lineages basal to the *E. lagostae* group.

Key words: taxonomy, morphology, molecular phylogeny, *COI, 16S rRNA*, distribution, ecology, Croatia, Bosnia and Herzegovina

Vignoli, V., Podnar, M., Kulijer, D. & Tvrtković, N.: Prvi sveobuhvatni opis hrvatskog endemskog politrihnog škorpiona *Euscorpius lagostae* Di Caporiacco, 1950 (Scorpiones, Euscorpiidae. Nat. Croat., Vol. 35, No. 2, _____, 2026, Zagreb.

U radu je detaljno opisana slabo istražena endemična vrsta Hrvatske *Euscorpius lagostae* Di Caporiacco, 1950 koja pripada kompleksu svojti *Euscorpius hadzii* Di Caporiacco, 1950, uz priložene fotografije morfoloških osobitosti te je potvrđena molekularnom filogenetskom analizom na većem uzorku. Uz podatke o novim nalazima (zapadni dio poluotoka Pelješca i otok Hvar) opisani su i ekološki uvjeti nalazišta ove zapostavljene vrste. Ovaj prilog je ujedno prvi korak u rasvjetljavanju taksonomskog statusa genetički srodnih svojti poznatih iz obalnog područja od ušća rijeke Neretve do granice s Crnom

* corresponding author

Gorom, uključivši jugoistočnu obalu Pelješca, otok Lokrum, otok Mljet i prekogranični dio južne Hercegovine. Među novoprikupljenim uzorcima škorpiona iz okolice Višegrada u sjeveroistočnim Dinaridima (BiH) te uz obalu Jadrana u blizini ušća Neretve (Hrvatska) utvrđene su duboko divergentne genetičke linije, bazalne u odnosu na *E. lagostae* i srodne svojte.

Ključne riječi: taksonomija, morfologija, molekularna filogenija, *COI*, *16S rRNA*, rasprostranjenost, ekologija, Hrvatska, Bosna i Hercegovina

INTRODUCTION

DI CAPORIACCO (1950) examined a sample of 15 specimens of "*Euscorpius carpathicus*" from Bosnia and Herzegovina, Montenegro and Croatia, characterized by a remarkably high number of trichobothria on pedipalp patella (DI CAPORIACCO, 1950). The author did not provide any taxonomic opinion on the juvenile specimen from Montenegro (Lovćen Mt. above Cattaro, now Kotor) but distinguished two morphotypes among the remaining samples. One large, fawn-coloured morphotype from Bosnia and Herzegovina (Ivan pass between Neretva and Bosna rivers, 950 m a.s.l.) was renamed *Euscorpius carpathicus hadzii* Di Caporiacco, 1950, and one smaller morphotype, with a "stockier appearance", from two Croatian islands, Meleda (now Mljet) and Lagosta (now Lastovo), was elevated to subspecies rank as *Euscorpius carpathicus lagostaes* Di Caporiacco, 1950. To support this taxonomic arrangement, the zoologist provided a short (thirteen lines) but clear description including morphological traits such as pectinal teeth count, metasomal carination and trichobothrial count (DI CAPORIACCO, 1950). Subsequently, the latter subspecies reappeared in the literature (BARTOLOZZI *et al*., 1987; LACROIX, 1991a; FET *et al*., 2000; VIGNOLI & SALOMONE, 2008) only as a citation and without the "s" in the subspecies name: *Euscorpius carpathicus lagostae* Di Caporiacco, 1950. Only after 52 years were both subspecies re-examined as part of elevating *Euscorpius hadzii* Di Caporiacco, 1950 to the species rank (FET & SOLEGLAD, 2002). The authors did not find the type specimen of *E. c. hadzii* from Bosnia and Herzegovina (Ivan pass), and selected a neotype from the more distant Albania (Prokletije Mts.), a choice that conflicts with ICZN rules. Although the two examined *E. c. lagostae* syntypes from the Adriatic islands present a diagnostic pedipalp trichobothria count (partly overlapping with *E. hadzii* specimens distributed from the Adriatic islands to Bulgaria sensu FET & SOLEGLAD, 2002), as well as a thinner metasomal segment V, smaller size, different coloration and pedipalp chela carination, the authors placed *E. c. lagostae* as synonym of *E. hadzii* probably due to the limited material examined.

Later FET *et al*. (2014), following molecular and morphological analyses, described within the *E. hadzii* complex the new species *E. solegladi* Fet, Graham, Webber & Blagoev, 2014, distributed in Bulgaria and Greece, and noted that samples from Bosnia and Herzegovina represent a different taxon from Albanian *E. hadzii* s.s. In a recent extensive molecular study of eastern Adriatic euscorpiids, PODNAR *et al*. (2021) confirmed two main groups within the former *E. hadzii*. The first group (Eh1) included *E. lagostae* from Lastovo Island, and another subgroup probably represents a distinct taxon distributed along the coast around Dubrovnik, with one locality in Bosnia and Herzegovina south of Trebinje. The second group (Eh2) comprised *E. hadzii* from the *terra typica* in the Prokletije Mts., *E. solegladi* in Albania and probably two unnamed montane taxa (Eh2a, Eh2b) from Montenegro and Bosnia and Herzegovina. Višnjeva near Bar on the Adriatic coast of Montenegro (GRAHAM *et al*., 2012: "Višnjevo") was incorrectly

designated on the map within the Prokletije Mts. in PODNAR *et al*. (2021). The authors underlined a clearly distinct phylogenetic lineage of *E. hadzii* from Lastovo Island, confirming that group Eh1 represents the sister lineage to *E. hadzii* sensu FET & SOLEGLAD (2002). Based on clear morphological differences between (i) *E. hadzii* neotype together with three additional Albanian specimens presented in FET & SOLEGLAD (2002) and (ii) the available specimens from Lastovo Island, PODNAR *et al*. (2021) elevated the former island subspecies to species rank as *Euscorpius lagostae* Di Caporiacco, 1950. The taxonomic rearrangement lacked detailed morphological analysis, but the authors highlighted that it would be addressed within ongoing investigation of the Balkan scorpiofauna once a larger sample became available. Based on a larger sample of freshly collected specimens obtained during the 2024 field expedition in southern Croatia, together with additional available material, including several specimens from Bosnia and Herzegovina collected by Dejan Kulijer, we provide a detailed phylogenetic analysis and redescription of this poorly studied species, accompanied by the first morphological illustrations. New distribution data and ecological aspects are provided.

MATERIAL AND METHODS

DNA extraction, PCR amplification and sequencing

Genomic DNA was extracted from a single leg, and fragments of the mitochondrial cytochrome c oxidase subunit 1 gene (*COI*; DNA barcode region; HEBERT *et al*., 2003) and mitochondrial *16S* rRNA (*16S*) were amplified and sequenced for 18 and 11 specimens, respectively (Tab. S1), following PODNAR *et al*. (2021). *COI* sequences were deposited in BOLD (RATNASINGHAM & HEBERT, 2007), and *16S* sequences in GenBank.

Sequence editing, alignment and genetic distance analysis

Sequences were inspected, edited, and aligned in BioEdit v. 7.2.5 (HALL, 1999). Intra- and inter-clade *COI* p-distance ranges were calculated in MEGA v. 11 (TAMURA *et al*., 2021) with missing data treated using both complete and pairwise deletion options.

Phylogenetic analysis

Bayesian inference was performed in MrBayes v. 3.2.7a (HUELSENBECK & RONQUIST, 2001; RONQUIST & HUELSENBECK, 2003) on Dataset 1 and Dataset 2 using two parallel runs of four chains each for 5,000,000 generations, sampling every 1,000 generations, with the first 1,000 samples discarded as burn-in. Along with newly obtained *COI* sequences, Dataset 1 comprised previously published DNA barcodes of the *Euscorpius hadzii* species complex, as well as sequences of several related *Euscorpius* species retrieved from BOLD. Dataset 2 comprised concatenated *COI* and *16S* sequences from this and previous studies (Tab. S1). Sequences of *Tetratrichobothrius flavicaudis* (De Geer, 1778) were used as an outgroup. Dataset 1 was partitioned by codon position, whereas Dataset 2 was partitioned by gene and codon position, with substitution models for each partition selected in jModelTest2 (DARRIBA *et al*., 2012) under the Bayesian information criterion (BIC).

Phylogeographic analysis

A median-joining (MJ) haplotype network (BANDELT *et al*., 1999) of mitochondrial *COI* haplotypes belonging to the Eh1a and Eh1b clades of the *Euscorpius hadzii* species complex (Croatian Adriatic coast and islands, Fig. 5 in PODNAR *et al.*, 2021) was constructed using PopART v. 1.7 (LEIGH & BRYANT, 2015).

Species delimitation

Species delimitation within the *E. hadzii* species complex was assessed using an integrative approach combining two distance-based methods: ABGD (PUILLANDRE *et al*., 2012) and ASAP (PUILLANDRE *et al*., 2021) along with two tree-based methods: bPTP (ZHANG *et al*., 2013) and mPTP (KAPLI *et al*., 2017), as implemented in iTAXOtools (VENCES *et al*., 2021). ABGD and ASAP analyses were performed using Kimura 2-parameter distances; default parameters were applied, with X set to 1.2 for ABGD. The Bayesian consensus tree was used as input for the bPTP analysis, whereas the maximum-likelihood (ML) tree inferred in IQ-TREE with automatic model selection under default settings was used for the mPTP analysis.

Divergence time estimation

A time-calibrated tree was inferred in BEAST v. 2.7.7 on the CIPRES Science Gateway (MILLER *et al*., 2010) based on *COI* and *16S* alignments from Dataset 2 under a strict molecular clock and a Yule speciation prior. The dataset was partitioned by gene, with *COI* additionally partitioned by codon position and selected substitution models (jModelTest2; DARRIBA *et al*., 2012) were applied. The applied calibration scheme corresponds to Calibration I of PODNAR *et al*. (2021): the *COI* substitution rate was set to a mean of 0.0134 substitutions/site/Myr (range 0.01-0.0174) following PODNAR *et al.* (2021), and the *16S* rate to a mean of 0.005 substitutions/site/Myr (range 0.002-0.008) following GANTENBEIN & LARGIADÈR (2002) and ŠTUNDLOVÁ *et al*. (2019). The MCMC analysis was run for 100 million generations, sampling every 10,000 generations, with the first 10% of samples discarded as burn-in.

Morphology, map and abbreviations

Morphological descriptive terms follow: HJELLE (1990) for general morphology; STAHNKE (1970) for carapace; LORIA & PRENDINI (2014) for lateral ocelli; SOLEGLAD & SISSOM (2001) for cheliceral dentition; SOLEGLAD & FET (2003) for sternum; VACHON (1974) for trichobothria pattern, GONZÁLEZ-SANTILLIÁN & PRENDINI (2013) for pedipalp chela and metasoma carinae; KOVAŘIK & ŠT'ÁHLAVSKÝ (2020) for pedipalp shape, and BLASCO-ARÓSTEGUI & PRENDINI (2023) for hemispermatophore. Morphology was studied under stereomicroscope (Euromex Z1654), and all measurements are in mm taken with an ocular micrometer following TROPEA *et al.* (2014) and CAIN *et al.* (2021). Carination and morphosculpture analysis were conducted under UV light (VOLSCHENK, 2005). Colors have been determinate on live specimens using NCS - Natural Colour System®© (NCS Scandinavian Colour Institute, Stockholm, Sweden) under a 1.600 lumen led lamp (5600-6500 K). Illustrations were prepared both under UV and visible light using a Fujifilm X-T2 digital camera equipped with a Laowa 25 mm and 65 mm lens. Fieldwork was conducted during the day and night with ultraviolet (UV) lamps. All specimens are preserved in 75-95% ethanol. Geographical coordinates were taken with a Garmin GPS device. Distribution

map was produced using QGIS version 3.40.6. Used abbreviations: **CNHM** = Croatian Natural History Museum (Hrvatski prirodoslovni muzej), Zagreb, Croatia; **ZMBH** = Zemaljski muzej Bosne i Hercegovine (National Museum of Bosnia and Herzegovina), Sarajevo, Bosnia and Herzegovina; **MZUF** = Museo Zoologico La Specola, Università di Firenze, Italy; **VVZC** = Valerio Vignoli Zoological Collection, Siena, Italy; Pe = pedipalp patella external; Pv = pedipalp patella ventral; L= left; R = right. The samples examined morphologically are deposited in CNHM, MZUF and VVZC collections.

Comparative material

In addition to the examined material used for the redescription, morphological traits of the following specimens were observed: *Euscorpius hadzii* Di Caporiacco, 1950, **VVZC**: 2 adult ♂♂ (VVZC221, VVZC222), Boga (Bogë), northern Albania (close to *terra typica*), 42°23′53″N 19°38′44″E, 1300-1400 m a.s.l., 15.VIII.1993, Giuliano Trezzi leg.; *Euscorpius* aff. *hadzii*, **ZMBH**: 1 adult ♀ (ZMBH151), Rujište, ski trail, Prenj Mt., Bosnia and Herzegovina, 43°27'46''N, 17°57'44''E, 1600 m a.s.l., 29.VII.2017, Dejan Kulijer leg.; *Euscorpius* sp. 1 second instar young (VVZC2411), Smrden grad fortress above Klek, Southern Croatia, 42°57'02.6"N 17°33'59.1"E, 222 m a.s.l., 15.IX.2024, V. Vignoli, N. Tvrtković, D. Kulijer leg.; *Euscorpius carpathicus lagostae* Di Caporiacco, 1950, **MZUF**: 1 adult ♂ (lectotype 72/5968), 1 adult ♀ (paralectotype 72/5969), Lastovo Island, Southern Croatia, 02.IV.1936, leg. unknown.

RESULTS

Molecular analyses: phylogeny, divergence dating, phylogeography, species delimitation, and genetic distance analysis

COI alignments used for phylogenetic and phylogeographic analyses were 649 bp long, with selected models for the 1st, 2nd and 3rd codon positions being K2P, F81 and HKY+G in Dataset 1 and HKY, HKY and HKY+G in Dataset 2, respectively. The *16S* alignment was 400 bp long, and the best-fit model was HKY+G.

Bayesian phylogenetic inference based on Dataset 1 (Fig. 2a) recovered all *COI* sequences of the *Euscorpius hadzii* complex within a highly supported monophyletic clade. Newly obtained samples from Mljet Island (Fig. 1) clustered within the well-supported coastal Eh1a clade, whereas samples from Hvar Island and the distal western part of the Pelješac Peninsula grouped within the Eh1b clade together with samples from Lastovo Island. Both are members of the *E. hadzii* 1 group; however, the sister relationship between the Eh1a and Eh1b clades is now only moderately supported by Bayesian posterior probabilities (PP = 0.96). Four newly sequenced samples from the eastern Dinarides (Prenj, Kalinovik, Konjic, and Foča) were recovered within the well-supported Eh2a clade, which likely represents a putative new species (see below). The former Eh2c clade (PODNAR *et al.*, 2021) was not recovered; instead, the subclades Eh2a + Eh2b (corresponding to *E.* aff. *hadzii*), Eh2d (*E. hadzii*), and Eh2e (including specimens identified as *E. solegladi*) form an unresolved trichotomy. Additionally, two newly sequenced samples from the Višegrad area (border area of NE Bosnia and Herzegovina, close to Serbia) cluster with moderate support as sister lineage to all afore mentioned Eh clades. Finally, the sample from Klek (Croatia) represents the most basal lineage within the *E. hadzii* species complex, indicating an early divergence within this group.

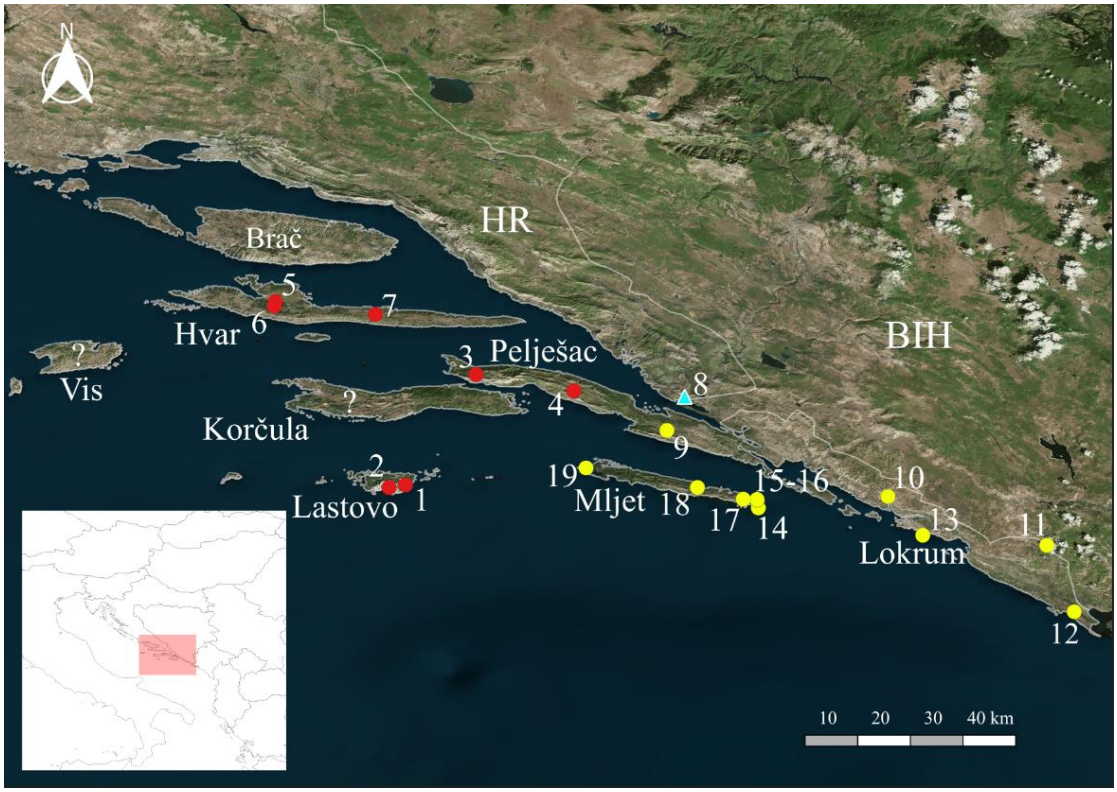

Fig. 1. Distribution of known locality records. A) *Euscorpius lagostae* group (Eh1b): *E. lagostae* Di Caporiaco, 1950 (red circles): (**1**) Rača cave entrance; (**2**) Uska bay; (**3**) Nakovana; (**4**) Donja Banda, Potomje, quarry; (**5**) Dol (near Stari Grad); (**6**) Dol Sv. Nikola peak; (**7**) Zastražišće. B) *Euscorpius* sp. (*E. hadzii* complex): basal lineage (blue triangle): (**8**) Klek; Smrden grad. C) *Euscorpius* aff. *lagostae* group (Eh1a): (yellow circles): (**9**) Deveterica vertical cave entrance; (**10**) Ljubač; (**11**) 15 km S of Trebinje (BIH); (**12**) Vitaljina; (**13**) Lokrum Island near Dubrovnik; and locality records from Mljet Island (**14**) Blaće, Saplunara; (**15**) Stražište hill (trail Sv. Pavla); (**16**) Korita, N of Radino brdo hill; (**17**) Korita, Sv. Gospa od Brijega); (**18**) Sobra; (**19**) Kulijer near Pomena. Specimens from Vis and Korčula islands, NHMW, designated as *E. hadzii* by FET & SOLEGLAD (2014) are marked with question marks (?). These are probably *E. lagostae* but require re-examination of the material in the NHMW collection.

The BEAST time-calibrated tree (*COI* + *16S*) (Fig 2b) was largely congruent with the *COI* Bayesian tree (Fig. 2a) in recovering the same major clades within the *E. hadzii* complex. However, deeper relationships differed: the BEAST topology recovered an Eh2c node uniting Eh2d and Eh2e and grouped the Klek and Višegrad samples within the same well-supported lineage, sister to the Eh1 group, rather than as the most basal lineages within *E. hadzii* species complex as recovered in the *COI* tree. Bayesian inference based on the same combined dataset (*COI* + *16S*) yielded a topology congruent with the BEAST tree within the *E. hadzii* species complex (Fig. S1). The divergence time between basal lineages (Klek and Višegrad) and Eh1 group were 3.68 Ma (95% HPD: 5.69-2.37). The estimated divergence times within Eh1 group were 2.23 Ma (95% HPD: 3.48-1.34) for the Eh1a lineage and 0.71 Ma (95% HPD: 1.21 - 0.32) for Eh1b, whereas the basal Visegrad - Klek lineages diverged somewhat earlier at 2.63 Ma (95% HPD: 4.19 - 1.53).

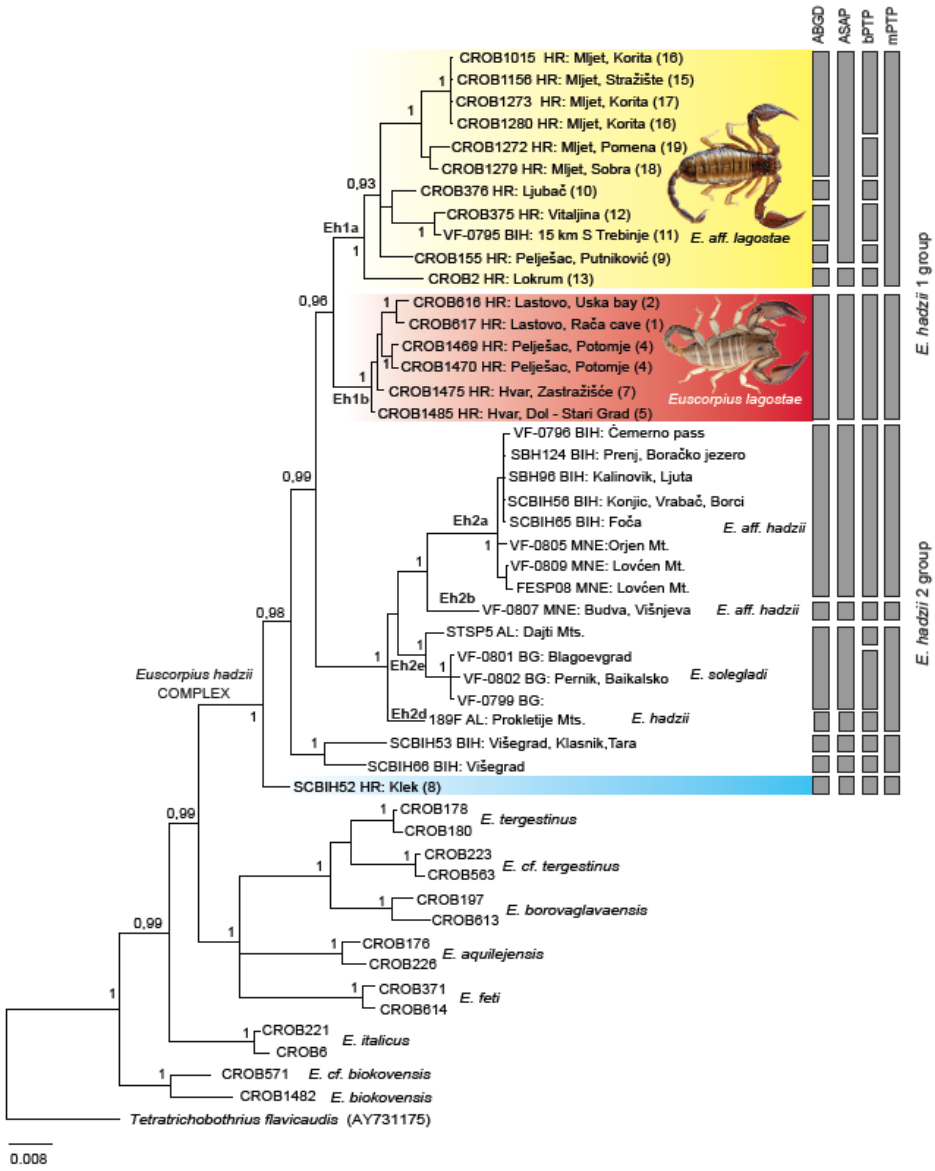

Fig. 2a. Bayesian phylogram based on mitochondrial *COI* sequences showing the results of species delimitation analyses. Numbers at nodes indicate Bayesian posterior probabilities. Grey blocks represent delimited units inferred by ABGD, ASAP, bPTP, and mPTP analyses and are shown adjacent to the corresponding terminal clades. Numbers in parentheses correspond to sampling localities shown in the maps.

Eh2 group began diversifying at 3.21 Ma (95% HPD: 5.23 - 1.84), and within it, the recently diverged Eh2a clade has an estimated age of 0.36 Ma (95% HPD: 0.72 - 0.11). The crown age of the *E. hadzii* complex (including *E. salentinus* Tropea, 2017) estimated at 4.93 Ma (95% HPD: 7.53 - 3.13).

In the median-joining network (Fig. 3), genetically closely related *Euscorpius lagostae* haplotypes from Hvar Island, Lastovo Island, and the distal western part of the Pelješac Peninsula are contained within a clearly delimited subclade (Eh1b). Although forming a single

genetic cluster, these haplotypes exhibit pronounced geographic structuring. In contrast, haplotypes belonging to the Eh1a clade do not form a single coherent subnetwork but are instead divided into five genetically divergent and geographically structured subnetworks, corresponding to populations from Mljet Island, landward part of the Pelješac Peninsula, as well as Lokrum Island, the Dubrovnik coast, and the Konavle region and southern Herzegovina.

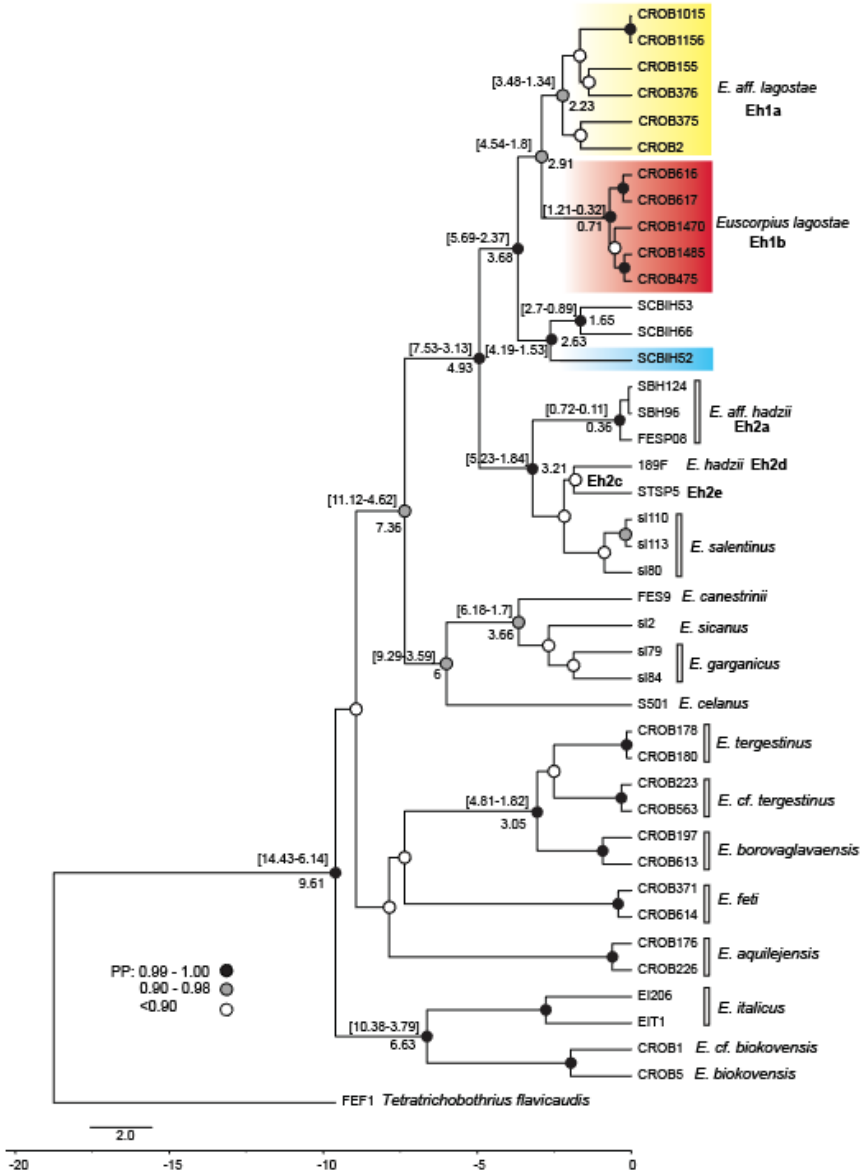

Fig. 2b. Time-calibrated BEAST gene tree inferred from mitochondrial *COI* and *16S* sequences. Numbers at nodes indicate median divergence time estimates, with values in brackets representing the 95% highest posterior density (HPD) intervals. Node support is indicated by Bayesian posterior probabilities (PP), categorised as shown in the legend.

Species delimitation analyses yielded different numbers of putative species depending on the method used (Fig. 2a). The distance-based ABGD analysis recovered a stable partition of 13 molecular operational taxonomic units (MOTUs) across a wide range of prior intraspecific

divergence values, whereas ASAP supported a more conservative optimal delimitation of 10 MOTUs. Among tree-based approaches, bPTP inferred the highest number of putative species (15), while the most conservative delimitation was obtained with mPTP (10 MOTUs). Despite differences in the total number of delimited units, all methods consistently recovered the same major lineages, differing primarily in the degree of subdivision within these lineages. According to the most conservative mPTP delimitation, all members of the Eh1a clade are interpreted as a single species (*E.* aff. *lagostae*), whereas all applied methods support the recognition of the Eh1b clade (*E. lagostae*).

The ranges of uncorrected pairwise genetic distances (p-distances) in the DNA barcode region of mt *COI* gene are shown in Tab. 1. Eh1a (*E.* aff. *lagostae*) and Eh1b (*E. lagostae*) differ by 3.5-5.2%, which exceeds the intraspecific genetic distances observed within *E. lagostae* but overlaps with intraclade divergence within Eh1a, specifically between the Mljet and Lokrum lineages and the mainland populations. The genetic distance between two other valid species belonging to the *E. hadzii* species complex (Tab. 1), *E. hadzii* (Eh2d) and *E. solegladi*, ranges from 3.6 to 3.8%. This divergence is comparable to or lower than that observed between Eh1a (*E. lagostae*) and Eh1b and is also lower than some intraclade distances within Eh1a, particularly between the Lokrum lineage and all other investigated *E. lagostae* aff. populations (3.9-4.9%).

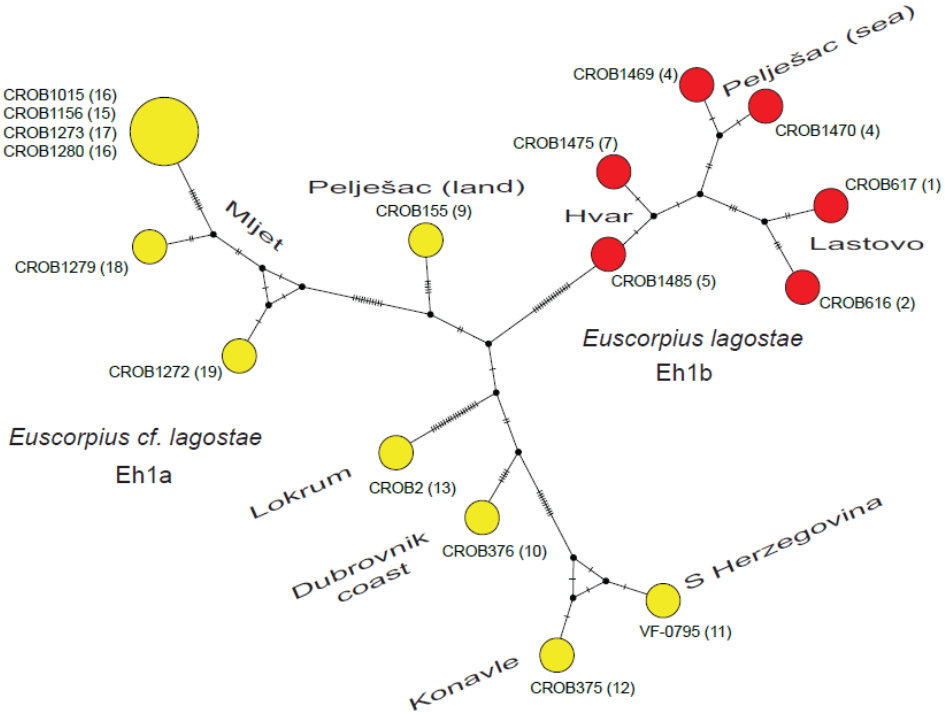

Fig. 3. Median-joining network of mitochondrial *COI* haplotypes belonging to the Eh1a and Eh1b clades (Fig. 2) of the *Euscorpius hadzii* species complex. Circle size is proportional to haplotype frequency, tick marks indicate the number of mutational steps, and small black circles represent median vectors. Numbers in parentheses correspond to sampling localities shown in the maps. land = landward; sea = seaward.

Tab. 1. Ranges of uncorrected pairwise genetic distances (p-distances) based on the DNA barcode fragment of the *COI* gene. Upper values were calculated using the pairwise deletion option for missing data (649 positions), whereas lower values were obtained using the complete deletion option (525 positions). Abbreviations: Elag = *E. lagostae*, STSP = STSP5 (Eh2e), Esole = *E. solegladi*.

	Mljet	Putnik	Ljubač	Vitaljina	Lokrum	Elag	Eh2a	Eh2b	Eh2d	STSP	Esole	Višegrad	Klek
Mlj	0.9–1.8 1.0–2.1	2.8–3.5 2.9–3.8	3.4–4.0 3.8–4.6	3.2–4.0 3.2–4.0	4.2–4.9 4.4–5.3	3.5–5.2 4.0–5.9	6.0–7.2 6.5–7.2	7.7–8.2 7.4–8.0	6.3–6.8 6.5–7.0	5.8–6.1 5.7–6.1	5.7–6.0 5.5–6.3	4.9–5.5 4.8–5.5	4.9–5.7 4.6–5.5
Put	2.8–3.5 2.9–3.8	–	2.3–2.3 2.3–2.3	3.4–3.4 2.9–2.9	4.0–4.0 4.0–4.0	3.5–4.2 3.4–4.2	6.6–7.2 6.7–7.2	7.2–7.2 6.7–6.7	6.1–6.1 6.3–6.3	5.8–5.8 5.7–5.7	5.5–5.9 5.1–5.3	4.3–4.6 4.0–4.2	4.9–4.9 4.4–4.4
Ljub	3.4–4.0 3.8–4.6	2.3–2.3 2.3–2.3	–	2.6–2.6 2.5–2.5	4.0–4.0 4.2–4.2	3.7–4.6 3.8–5.0	6.3–7.0 6.5–7.2	7.7–7.7 7.6–7.6	6.4–6.4 6.7–6.7	6.1–6.1 6.1–6.1	6.2–6.2 6.1–6.3	4.9–5.2 5.0–5.5	4.9–4.9 4.8–4.8
Vita	3.2–4.0 3.2–4.0	3.4–3.4 2.9–2.9	2.6–2.6 2.5–2.5	0.5–0.5 0.4–0.4	3.9–3.9 4.0–4.0	3.5–4.6 3.6–4.8	6.0–6.5 6.1–6.5	7.2–7.6 7.0–7.4	6.1–6.1 6.3–6.3	6.3–6.3 6.3–6.3	6.3–6.8 6.3–6.5	5.1–5.7 5.0–5.3	4.8–5.1 4.2–4.6
Lokr	4.2–4.9 4.4–5.3	4.0–4.0 4.0–4.0	4.0–4.0 4.2–4.2	3.9–3.9 4.0–4.0	–	4.3–5.2 4.6–5.7	7.4–7.9 7.4–7.8	7.4–7.4 7.0–7.0	6.8–6.8 7.0–7.0	6.7–6.7 6.7–6.7	6.8–6.8 6.3–6.5	5.7–6.3 5.9–6.1	4.8–4.8 4.4–4.4
Elag	3.5–5.4 4.0–5.9	3.5–4.5 3.4–4.4	3.7–4.6 3.8–5.0	3.5–4.6 3.6–4.8	4.3–5.2 4.6–5.7	0.3–1.4 0.2–1.5	6.3–8.1 6.7–8.2	6.6–7.6 6.5–7.4	5.0–6.1 5.1–6.3	5.6–6.8 5.5–6.9	5.5–6.6 5.3–6.7	4.0–5.7 3.8–5.7	3.9–5.1 3.6–5.1
Eh2a	6.0–7.2 6.5–7.2	6.6–7.2 6.7–7.2	6.3–7.0 6.5–7.2	6.0–6.5 6.1–6.5	7.4–7.9 7.4–7.8	6.3–8.1 6.7–8.2	0.2–0.9 0.2–0.8	4.6–4.8 4.6–4.8	5.4–5.7 5.5–5.7	5.3–5.6 5.3–5.5	4.9–6.0 5.7–6.1	7.1–7.9 7.0–7.8	6.9–7.3 6.9–7.2
Eh2b	7.7–8.2 7.4–8.0	7.2–7.2 6.7–6.7	7.7–7.7 7.6–7.6	7.2–7.6 7.0–7.4	7.4–7.4 7.0–7.0	6.6–7.4 6.5–7.2	4.6–4.9 4.6–4.8	–	4.1–4.1 4.0–4.0	4.3–4.3 4.4–4.4	4.6–4.6 4.4–4.6	6.5–8.0 6.3–7.6	6.6–6.6 6.9–6.9
Eh2d	6.3–6.8 6.5–7.0	6.1–6.1 6.3–6.3	6.4–6.4 6.7–6.7	6.1–6.1 6.3–6.3	6.8–6.8 7.0–7.0	5.0–6.1 5.1–6.3	5.4–5.7 5.5–5.7	4.1–4.1 4.0–4.0	–	3.4–3.4 3.4–3.4	3.6–3.8 3.6–3.8	6.8–6.8 6.7–6.9	6.1–6.1 5.9–5.9
STSP	5.8–6.1 5.7–6.1	5.8–5.8 5.7–5.7	6.1–6.1 6.1–6.1	6.3–6.3 6.3–6.3	6.7–6.7 6.7–6.7	5.6–6.8 5.5–6.9	5.3–5.6 5.3–5.5	4.3–4.3 4.4–4.4	3.4–3.4 3.4–3.4	–	1.6–1.8 1.3–1.5	6.5–6.8 6.3–6.5	6.3–6.3 5.9–5.9
Esole	5.7–6.0 5.5–6.3	5.5–5.9 5.1–5.3	6.2–6.2 6.1–6.3	6.3–6.8 6.3–6.5	6.8–6.8 6.3–6.5	5.5–6.6 5.3–6.7	4.9–6.0 5.7–6.1	4.6–4.6 4.4–4.6	3.6–3.8 3.6–3.8	1.6–1.8 1.3–1.5	0.3–0.3 0.2–0.2	6.0–6.8 6.1–6.7	6.2–6.2 5.9–6.1
Višeg	4.9–5.5 4.8–5.5	4.3–4.6 4.0–4.2	4.9–5.2 5.0–5.5	5.1–5.7 5.0–5.3	5.7–6.3 5.9–6.1	4.0–5.7 3.8–5.7	7.1–7.9 7.0–7.8	6.5–8.0 6.3–7.6	6.8–6.8 6.7–6.9	6.5–6.8 6.3–6.5	6.0–6.8 6.1–6.7	3.7–3.7 3.0–3.0	3.9–4.3 4.0–4.0
Klek	4.9–5.7 4.6–5.5	4.9–4.9 4.4–4.4	4.9–4.9 4.8–4.8	4.8–5.1 4.2–4.6	4.8–4.8 4.4–4.4	3.9–5.1 3.6–5.1	6.9–7.3 6.9–7.2	6.6–6.6 6.9–6.9	6.1–6.1 5.9–5.9	6.3–6.3 5.9–5.9	6.2–6.2 5.9–6.1	3.9–4.3 4.0–4.0	–

Systematic part

FAMILY EUSCORPIIDAE LAURIE, 1896

SUBFAMILY EUSCORPIINAE LAURIE, 1896

Genus *Euscorpius* Thorell, 1876

Subgenus *Euscorpius* Thorell, 1876

Euscorpius lagostae Di Caporiacco, 1950 (Figs. 4-25)

TYPE LOCALITY. Lastovo Island (based on lectotype, here designated).

HISTORICAL MENTIONS:

Euscorpius carpathicus lagostaes Di Caporiacco, 1950: (partim)

Euscorpius hadzii Caporiacco, 1950: FET & SOLEGLAD 2002 (partim)

Euscorpius lagostae Di Caporiacco, 1950: PODNAR *et al*. (2021)

LECTOTYPE DESIGNATION: Herewith we select one of syntype of *Euscorpius carpathicus lagostae* Di Caporiacco, 1950 as a lectotype. Namely, DI CAPORIACCO (1950) included specimens from both Lastovo and Mljet in his original description. Our molecular results clearly show that Mljet population hitherto regarded conspecific represents a distinct species. Because *"lagostae"* means "of Lastovo", we select Lastovo specimen as lectotype. The lectotype is deposited in Museo Zoologico La Specola, Università di Firenze, Italy (♂, MZUF 72/5968).

With respect to the citation of Ludovico Di Caporiacco as author, we noted that in some studies the citation was not used as recommended (LACROIX, 1991a; FET *et al*., 2000; FET & SOLEGLAD, 2002) since Italian names that begin with "di" need to be listed under this prefix (Council of Science Editors (CSE), 2006).

TYPE MATERIAL: Lectotype: 1 ♂ MZUF 72/5968, **Southern Dalmatia. Lastovo Island**, Croatia, 02.IV.1936.

OTHER TYPE MATERIAL: paralectotype 1 ♀ MZUF 72/5969, **Southern Dalmatia. Lastovo Island**, Croatia, 02.IV.1936.

EXAMINED MATERIAL. 22 specimens, Croatia. **Southern Dalmatia**. **Pelješac Peninsula**: 1 adult ♂ (VVZC2397), 2 adult ♀♀ (CNMH960, VVZC1914), 1 sub adult ♀ (VVZC2406), 1 juvenile ♀ (VVZC2408), 5 juvenile ♂♂ (VVZC2399, VVZC2400, VVZC2402, VVZC2403, VVZC2410), Nakovana (road to), 43°00'07''N, 17°04'51''E, 263 m a.s.l., 15.IX.2024, V. Vignoli, D. Lešić, M. Podnar, N. Tvrtković, D. Kulijer leg.; 1 adult ♀ (VVZC2394), 1 sub adult ♂ (VVZC2404), 1 juvenile ♀ (VVZC2407), 1 first instar young (VVZC2409), Donja Banda - Potomje (mine), 42°57'51.6"N 17°18'30.6"E, 273 m a.s.l., 15.IX.2024, V. Vignoli, N. Tvrtković, D. Kulijer leg., collected from the same locality as the DNA-barcoded samples CROB1469 and CROB1470 (Tab. S1). **Middle Dalmatia**. **Hvar Island**: 1 adult ♂ (VVZC2398), 1 juvenile ♂ (VVZC2401), Dol, entrance of village, 43°10'21''N, 16°36'52''E, 61 m a.s.l., 17.IX.2024; 4 adult ♀♀ (VVZC2395, VVZC2396, MZUF-INS-114048, CNHM961), 1 adult ♂ (CNHM962), 43°09'58''N, 16°37'09''E, 151 m a.s.l., 18.IX.2024, 1 first instar young (VVZC2405), 43°09'44''N, 16°36'43''E, 265 m a.s.l., 17.IX.2024, Dol, road to Sveti Nikola peak, V. Vignoli, N. Tvrtković leg.

DIAGNOSIS: Yellowish *Euscorpius* species with darker carapace, pedipalp chela and metasoma segments II-V. Tergites proximal portions lighter in color than remaining surface. Marbling on chelicera and metasoma segments II-V. Medium in size with adults reaching 35.4 mm in total length. Carapace long as wide with prominent lateral ocelli. Pedipalps with large, elongated chela (42-44% longer than carapace length) and femur longer than patella. Pedipalp fingers with margins type C (♂), linear in ♀. Polytrichous pedipalp patellar trichobothrial pattern: *eb*: 5, eb_{α}: 8, *esb*: 2, *em*: 5, *est*: 4, *et*: 9 (8-9); ventral aspect with 12 trichobothria. Number of pectinal teeth in ♂= 9, in ♀= 8. Weak metasomal carinae development, lateral median carina absent. Overall carination and granulation weak, similar in ♀ and ♂. Telson vesicle is not excessively developed in height with a length/height ratio of 1.87.

DESCRIPTION: The larger ♀ (VVZC1914) and ♂ (VVZC2397) were used for description; the only exception is for the study and illustration of the carapace of ♂ for which another male (VVZC2398) was observed, since this character is slightly damaged in specimen VVZC2397.

Morphometrics are provided in Tab. 2.

Color (Figs. 4-8, 25) Carapace, coxapophysis I-II, tergites, and metasoma segments I-V light brown (NCS S 5030-Y20R). Carapace distal portion darker, reddish brown (NCS S 8010-Y70R). Chelicera, posterior margins of tergites (I-VI), pectines and genital operculum, legs, pedipalp femur and patella intercarinal surfaces, and telson vesicle light ivory (NCS S 1020-Y10R). Pedipalp chela intercarinal surfaces, aculeus basal portion, ochre brown (NCS S 5040-Y40R). Pedipalp carinae and fingers, telson aculeus and leg ungues distal portion dark reddish brown (NCS S 8010-Y70R). Metasoma segments II-V and telson vesicle moderately marbled (NCS S 8010-G90Y) on ♀, while weakly marbled, only on segments IV-V, for ♂. Mesosoma intersegmental membranes are grey (NCS S 5502-G).

Chelicerae. Ventral distal denticle of movable finger longer than dorsal distal denticle; two small subdistal denticles, larger median denticle and one very small basal denticle, same in size as the proximal subdistal denticle. Ventral edge without denticles with brush-like setae on entire length. Dorsal surface of movable finger smooth with four setae. Fixed finger with four denticles: distal, subdistal and basal forming a bicusp; dorsal surface without setae. Manus dorsal surface smooth with 3 distal setae. Entirely (♀) and only distally (♂) moderately marbled, darker from proximal to distal portion; prolateral surface with brush-like setae while smooth on ventral and retrolateral portion.

Carapace (Figs. 9-10). Long as wide, acarinate with weak anterior median, posterior lateral and posterior marginal furrows; posterior median moderately deep. Dorsal surface finely granulated with larger granules on lateral margins, similar in the ♂. Anterior margin barely undulated as for posterior margin centrally weakly concave. Two pairs of prominent lateral ocelli, pattern type 2A, with mediolateral major (MLMa) ocelli larger than posterolateral major (PLMa) ocelli. Left mediolateral major ocellus is absent in ♀. Median ocular tubercle not very prominent with two median ocelli situated in anterior half of carapace and two macrosetae posteriorly to the ocelli.

Pedipalps (Figs. 11-18). *Coxa and trochanter*. Coxa with 4-3 moderate black brown spiniform granules on distal retrolateral portion, similar in size granules on prolateral edge and smaller distinct granules on dorsal and ventral edges. Dorsal and ventral with spiniform granules slightly smaller than for femur. All granules are darker than segment surfaces. *Femur*. Longer than patella and more than 2.5 (2.6 (♀) - 2.8 (♂)) times longer than width. Carination and granulation in ♀ as for ♂. Dorsal prolateral carina with black spiniform granules; dorsal retrolateral carina with similar granules but lighter in color and more distant between them. Retrolateral median carina well developed, 2/3 of segment length, and composed of distinct blunt orange brown rounded granules decreasing in size from distal to proximal portion. Retrolateral ventral carina incomplete with few granules on proximal portion; ventral prolateral carina as dorsal retrolateral carina. Prolateral median carina with distinct heterogeneous in size dark spiniform granules. All intercarinal surfaces finely granulated. *Patella*. Carination and granulation in ♀ as for ♂. All carinae orange-brown, darker than intercarinal surfaces. Dorsal prolateral carina costate-granular with sub-spiniform granules increasing in size from proximal to distal portion; dorsal retrolateral carina costate-granular with blunt granules (larger on distal portion), smooth. Retrolateral median carina wide with several blunt irregular and

heterogeneous in size granules. Ventral retrolateral carina costate-granular and ventral prolateral carinae similar but with more distinct blunt granules. Prolateral median carina absent. Dorsal intercarinal surface finely granulated with larger granules on distal portion. Prolateral intercarinal surface finely granulated with slightly larger granules on dorsal and ventral portions; dorsal patellar spur moderately developed with one basal macrosetae. Ventral intercarinal surface smooth with small granules on prolateral portion; retrolateral intercarinal surface smooth. *Chela*. Elongated chela, almost double (44%) in length than carapace length. Manus with dorsal prolateral carina costate-granular, proximal carina portion with two separated granules and with very low and distinct granules on entire carina. Dorsal retrolateral carina is also costate-granular and smooth, but with closer granules, more separated only on proximal distal end. Ventral prolateral carina like dorsal prolateral but with smaller granules. Ventral retrolateral carina has similar development as dorsal retrolateral but all granules are less merged with each other. Dorsal, prolateral and ventral median carina absent; retrolateral median carina incomplete with row of blunt granules from 2/3 of length till base of movable finger. All intercarinal surfaces sparsely setose, with marmoration macrosculpture and sparse small granules except ventral surface which is smooth. In the granulation no sexual dimorphism is evident. Fingers curved, more in ♂ with margins type C, linear in ♀. Movable finger in ♀ with shallow proximal and medial lobe, medial notch obsolete; fixed finger lobe and notches very similar to movable finger leaving a very little gap with closed fingers. Proximal and medial notch and medial lobe of movable finger moderately developed in ♂; fixed finger with deep and wide medial notch. Distal denticle similar in length on movable and fixed finger both in ♀ and ♂. Movable finger median denticle row with 6 subrows, 6 retrolateral accessory denticles in ♀, while 7 subrows and 7 retrolateral accessory denticles in ♂; 13 prolateral accessory denticles in both sexes. Fixed finger denticles are same in ♀ and ♂: median denticle row with 6 subrows, 6 retrolateral and 13 prolateral accessory denticles. Trichobothria pattern neobothriotaxic Type C. Femur with 3 trichobothria: Internal (*i*) trichobothria adjacent to dorsal prolateral carina. External trichobothria (*e*) included into dorsal retrolateral carina, while dorsal trichobothria (*d*) is close to this carina, but not surrounded by granules. Trichobothria *d* is located at the same distance between *e* and *i*. Patella with 47 (46 ♂) trichobothria: 2 dorsal: d_1-d_2; 1 prolateral (included into dorsal prolateral carina): *i*; 12 ventral: *v*; 32 (31 ♂) external: *eb* (5), eb_a (8), *esb* (2), *em* (4), *est* (4), *et* (9 (8 ♂)). Chela with 26 trichobothria. Chela manus with 18 trichobothria: 1 dorsal: *Dt*; 11 external: *Eb* (3), *Db*, *Esb*, v_4 (absent in ♀ R (Fig. 14) and in ♂ L), *Est*, *Et* (4); 2 internal: *ib*, *it*; 4 ventral: *V* (3), Et_1. Fixed finger with 8 trichobothria: 3 dorsal: *dt*, *dst*, *db*; and 5 externals: *et*, *est*, *dsb*, *esb*, *eb*. Trichobothria *est-dsb* distance is larger than *et-est* distance resulting in a *et-est/est-dsb* ratio of 0.8 (♀) and 0.77 (♂).

Sternum and genital operculum. Coxosternal region smooth with few sparse setae on coxapophysis and coxae of legs. Few darker small granules are present on prolateral portions of coxae. Sternum pentagonal shape, type 2 and long as wide. Entire surface is smooth except the distal margin which is granulated; distal and central areas with small setae and two larger setae on lateral lobes. Posterior emargination deep. Genital operculum divided longitudinally; smooth, shiny with few fine setae. Genital papillae externally visible (♂).

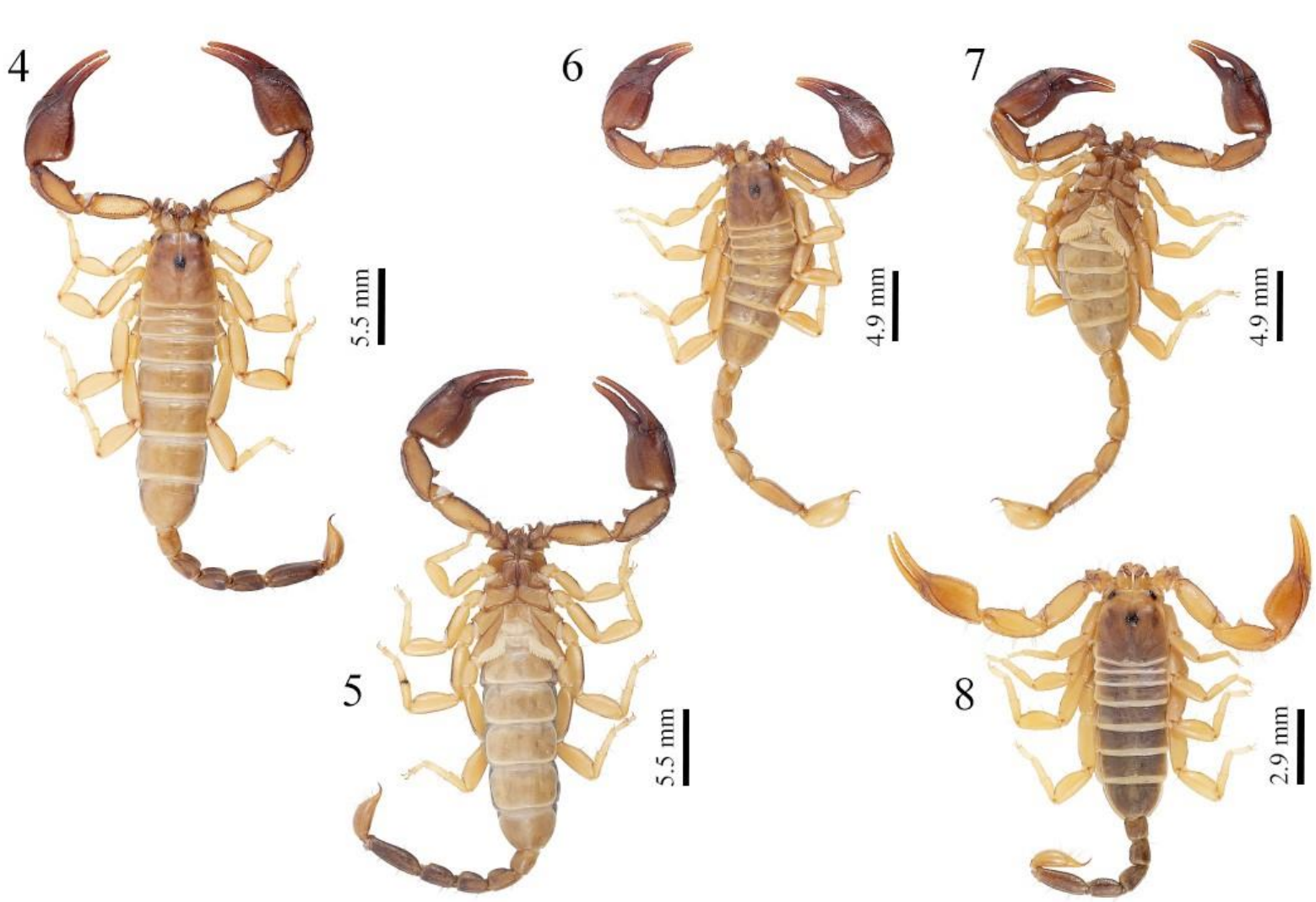

Plate 1, Figs. 4-8. *Euscorpius lagostae* Di Caporiacco, 1950: **Fig. 4.** Dorsal habitus, adult ♀ (VVZC1914). **Fig. 5.** Ventral habitus, adult ♀ (VVZC1914). **Fig. 6.** Dorsal habitus adult ♂ (VVZC2397). **Fig. 7.** Ventral habitus adult ♂ (VVZC2397). **Fig. 8.** Dorsal habitus of juvenile ♂ (VVZC2403).

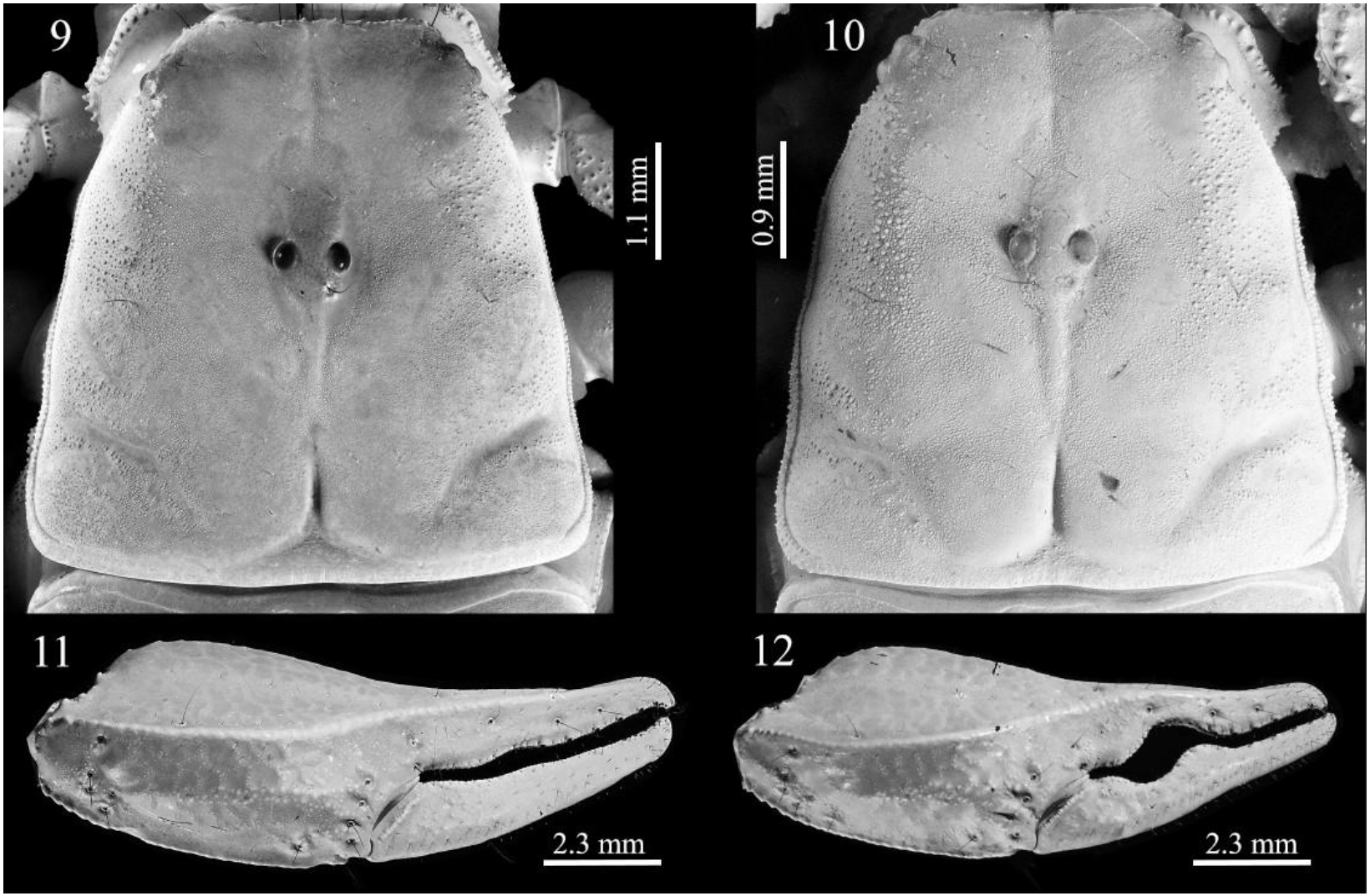

Plate 2, Figs. 9-12. *Euscorpius lagostae* Di Caporiacco, 1950: **Fig. 9.** Carapace dorsal aspect, adult ♀ (VVZC1914). **Fig. 10.** Carapace dorsal aspect, adult ♂ (VVZC2398). **Fig. 11.** Dorsal retrolateral aspect of pedipalp chela, adult ♀ (VVZC1914). **Fig. 12.** Dorsal retrolateral aspect of pedipalp chela, adult ♂ (VVZC2397).

Tab. 2. Measurements (mm) and pectinal teeth count of 10 analyzed adult specimens of *Euscorpius lagostae* Di Caporiacco, 1950. [1]CarA = Distance from center of median eyes to anterior carapace margin. [2]CarP = Distance from center of median eyes to posterior carapace margin. [3]Chela width = Wchel-A (TROPEA *et al*., 2014). In pedipalp total trochanter length is not included. Abbreviations: Car, carapace; Mes, mesosoma; Met, metasoma; Tel, telson.

		VVZC1914	VVZC2397	CNHM961	VVZC2395	VVZC2396	MZUF-INS-114048	VVZC2394	CNMH960	CNHM962	VVZC2398
		♀	♂	♀	♀	♀	♀	♀	♀	♂	♂
Carapace	anterior width:	2.4	2	2.2	2.2	2.1	2.2	1.9	2.2	1.9	1.7
	posterior width	5.4	4.8	5.6	5.1	5.3	5.5	4.7	5.2	4.4	4.3
	length:	5.5	4.9	5.4	5.3	5.4	5.4	4.8	5.2	4.5	4.3
	CarA[1]:	2.3	2.1	2.3	2.2	2.2	2.3	2	2.2	1.9	1.8
	CarP[2]:	3.2	2.8	3.1	3.1	3.2	3.1	2.8	3	2.6	2.5
Chela	width[3]:	3.3	3.1	3.4	3.2	3.1	3.4	2.7	3.2	2.8	2.8
	length:	9.9	8.8	9.7	9.4	9.5	9.9	8.3	9.4	8.1	7.9
	length movable finger	5.7	5	5.5	5.3	5.5	5.5	4.6	5.3	4.7	4.6
	length manus:	4.6	4.2	4.7	4.7	4.6	4.8	4.1	4.4	4	3.9
Patella	width:	1.9	1.7	1.9	1.9	1.6	1.9	1.6	1.8	1.5	1.5
	length:	4.4	4	4.4	4.4	4.2	4.5	3.8	4.3	3.8	3.6
Femur	width:	1.8	1.5	1.8	1.6	1.7	1.7	1.5	1.6	1.4	1.4
	length:	4.7	4.3	4.5	4.5	4.6	4.5	4.1	4.5	3.9	3.9
Pedipalp	length (trochanter not incl.):	19	17.1	18.6	18.3	18.3	18.9	16.2	18.2	15.8	15.4
Tergite I	length:	0.7	0.5	0.7	0.6	0.6	0.7	0.6	0.9	0.5	0.6
Tergite II	length:	1.2	0.9	1	1.1	1.1	0.7	0.9	1.2	0.7	0.7
Tergite III	length:	1.7	1.3	1.4	1.6	1.7	1.2	1.4	1.7	1	1.2
Tergite IV	length:	2.2	1.6	1.5	2.1	2.1	1.6	1.8	2	1.3	1.5
Tergite V	length:	2.4	1.8	1.7	2.4	2.4	1.7	1.9	2	1.4	1.7
Tergite VI	length:	2.5	1.8	1.9	2.5	2.5	1.8	2.1	1.8	1.5	1.8
Tergite VII	length:	2.9	2.1	2.4	2.9	3	2.2	2.4	2.3	2	2.3
Mesosoma	length (tergites)	13.6	10	10.6	13.2	13.4	9.9	11.1	11.9	8.4	9.8
Metasoma I	width:	1.6	1.6	1.7	1.6	1.6	1.6	1.4	1.6	1.4	1.4
	length:	1.6	1.7	1.6	1.6	1.6	1.6	1.4	1.6	1.5	1.5
	height:	1.4	1.3	1.3	1.2	1.4	1.3	1.1	1.3	1.2	1.2
Metasoma II	width:	1.4	1.4	1.4	1.3	1.4	1.3	1.2	1.4	1.3	1.2
	length:	1.9	2	1.9	1.9	1.9	1.9	1.6	1.9	1.9	1.8
	height:	1.4	1.3	1.4	1.3	1.3	1.4	1.2	1.4	1.2	1.2
Metasoma III	width:	1.4	1.3	1.3	1.3	1.3	1.2	1.2	1.3	1.2	1.2
	length:	2.1	2.2	2.1	2.1	2	2.2	1.8	2.1	2	2
	height:	1.4	1.3	1.4	1.3	1.3	1.3	1.2	1.3	1.2	1.2
Metasoma IV	width:	1.3	1.3	1.2	1.2	1.3	1.2	1.1	1.2	1.2	1.1
	length:	2.5	2.6	2.5	2.5	2.6	2.6	2.2	2.6	2.5	2.3
	height:	1.3	1.3	1.3	1.2	1.2	1.3	1.1	1.3	1.2	1.2
Metasoma V	width:	1.3	1.3	1.3	1.2	1.2	1.2	1.1	1.2	1.2	1.2
	length:	4.2	4.2	3.9	4	4	4.1	3.5	4.2	4	3.9
	height:	1.3	1.3	1.4	1.2	1.3	1.3	1.1	1.3	1.3	1.2
Metasoma I-V	length:	12.3	12.7	12	12.1	12.1	12.4	10.5	12.4	11.9	11.5
Vesicle	width:	1.3	1.7	1.3	1.2	1.2	1.3	1	1.2	1.4	1.5
	Length	2.8	3.4	2.7	2.6	2.6	2.7	2.4	2.7	3.1	3.1
	height:	1.3	1.8	1.3	1.2	1.3	1.3	1.1	1.3	1.7	1.6
Aculeus	length:	1.2	1.1	0.7	1.2	1.1	1.3	1.1	1.2	1.2	1.1
Telson	length:	4	4.5	3.4	3.8	3.7	4	3.5	3.9	4.3	4.2
Met +Tel	length:	16.3	17.2	15.4	15.9	15.8	16.4	14	16.3	16.2	15.7
Car+Mes+Met+Tel:	length:	35.4	32.1	31.4	34.4	34.6	31.7	29.9	33.4	29.1	29.8

Pectines. Basal piece with four setae. Marginal lamellae comprising three sclerites with several microsetae. Middle lamellae with six sclerites and with less setae than on marginal lamellae. Fulcra with 8 (♂) and 7 (♀) sclerites with few setae. Teeth with small setae on distal portion; count, 9-9 (♂) and 8-8 (♀).

Mesosoma. All tergites acarinate, surfaces I-VI slightly punctuated except central portions which are shagreened in ♀; for ♂ only the distal edge is punctuated while remaining surface is shagreened. Segment VII is both for ♀ and ♂ similar as for ♂ segments I-VI. Segment VII surface is with coarse granules on posterior margins, slightly stronger on ♂. Tergites I-VI with sparse macrosetae and two macrosetae on posterior margins. Sternites, surfaces III-VII smooth with small, elongated spiracles. Sparse macrosetae on all sternites more concentrated on lateral and posterior margins.

Legs: Coxa I-IV ventrally smooth with darker color rows of subspiniform granules on prolateral surfaces, larger on coxa III. Trochanter of legs I-III with small granules on dorsal surfaces and larger and darker granules on retrolateral edge; trochanter IV with similar granules, but only on dorsal edge. Femur of all legs with prolateral surfaces and retrolateral granulated, stronger on prolateral surfaces, but weaker on leg IV. Patella is smooth and similar in color as other segments except for the prolateral surface which is weakly marbled (only ♀) and with granules increasing in size from leg IV, almost smooth, to leg I. No sexual dimorphism is present on granulation. Tibial spur absent and two pedal spurs on all legs. Basitarsus with spinules on ventral surfaces of legs I-II (♂ L/R: I: 4/5, II: 4/2; ♀ L/R: I: 4/4, II: 4/4), while absent on legs III-IV. Telotarsus with one row of ventral and two distal lateral spinules (♂ L/R: I: 11/9, II: 9/10, III: 11/11, IV: 11/11; ♀ L/R: I: 10/8, II: 9/11, III: 11/11, IV: 11/9). Telotarsal ungues curved and pronounced dactyl. Sparse microsetae and macrosetae on all segments, more on basitarsus and telotarsus.

Metasoma and telson (Figs. 19-21): Dorsal lateral carinae with few granules on proximal portion of segment I, slightly larger on entire segment length on segments II-IV and more spiniform at the distal portion; very small and larger on proximal portion than on distal portion on segment V. Lateral median carina absent. Ventral lateral carinae absent on segment I, vestigial on segment II, obsolete on segment III and weak on segment IV; segment V with small subspiniform granules (largest granules of metasoma) increasing in size from basal to distal portion. Ventral median carina absent on segments I-II and vestigial on segments III-IV and weak with several small rounded and subspiniform granules, slightly larger on distal portion on segment V. This carina is linear with a small distal enlargement forming a "V". Dorsal intercarinal surfaces of all segments are shagreened. Lateral intercarinal surfaces finely shagreened, with few larger rounded granules on dorsal-distal portions on segments I-IV. Ventral intercarinal surfaces smooth, punctuated on segment I, while finely shagreened on segments II-IV; several sparse small, rounded granules on entire surface of segment V. Ventral and lateral surfaces with macrosetae. Carination and granulation are similar in ♀ and ♂. Anal arch with very small, rounded granules and 1 subspiniform granule on both lateral ends. Telson vesicle swollen in ♂ (almost 28% higher in height than for ♀) and elongated (twice the height), high as wide in ♀. All surfaces finely shagreened, slightly more developed in ♂, especially on distal ventral portion with one central larger granule. Sparse macrosetae and microsetae on ventral and lateral surfaces, most between distal vesicle margin and proximal aculeus margin. Annular ring absent in ♀, developed in ♂. Aculeus more curved in ♂ than in ♀. Marbling is weakly present on vesicle in ♀, absent in ♂.

Hemispermatophore (Figs. 22-24). To preserve the here described ♂, another adult ♂ has been dissected for observation (VVZC2398). Total length of left hemispermatophore is 5.7 mm.

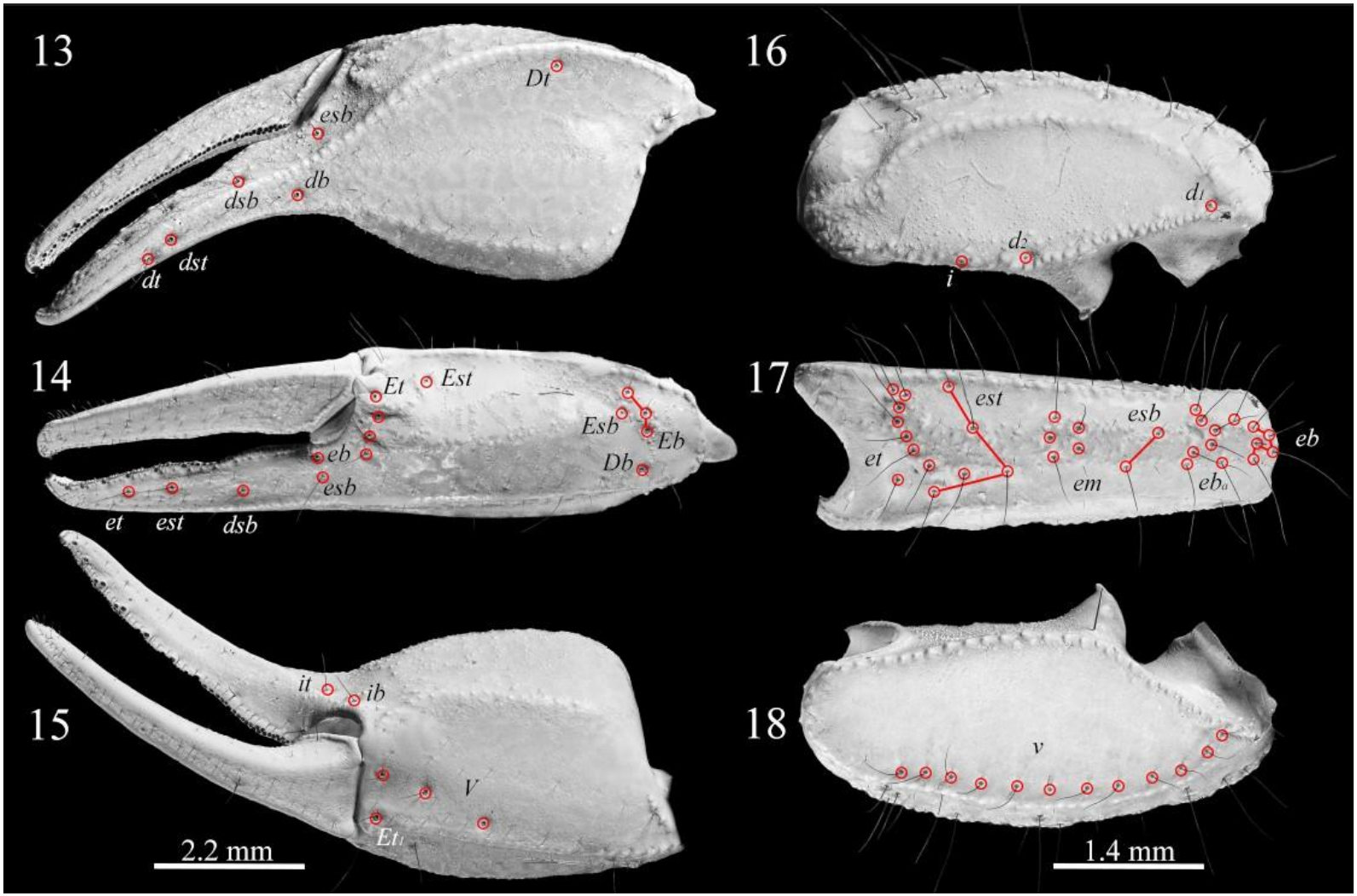

Plate 3, Figs. 13-18. *Euscorpius lagostae* Di Caporiacco, 1950: adult ♀ (VVZC1914): **Fig. 13.** Dorsal aspect of dextral pedipalp chela. **Fig. 14.** Retrolateral aspect of pedipalp chela. **Fig. 15.** Ventral aspect of pedipalp chela. **Fig. 16.** Patella dorsal aspect. **Fig. 17.** Patella retrolateral aspect. **Fig. 18.** Patella ventral aspect. Abbreviations: *d*, dorsal; *Db*, *db*, dorsal basal; *dsb* dorsal suprabasal; *dst* dorsal subterminal; *Dt*, *dt*, dorsal terminal; *e*, external; *Eb*, *eb*, external basal; *eba*, external basal-a; *em*, external medial; *Esb*, *esb*, external suprabasal; *Est*, *est*, external subterminal; *Et*, *et*, external terminal; *i*, internal; *ib*, internal basal; *it*, internal terminal; *V*, *v*, ventral.

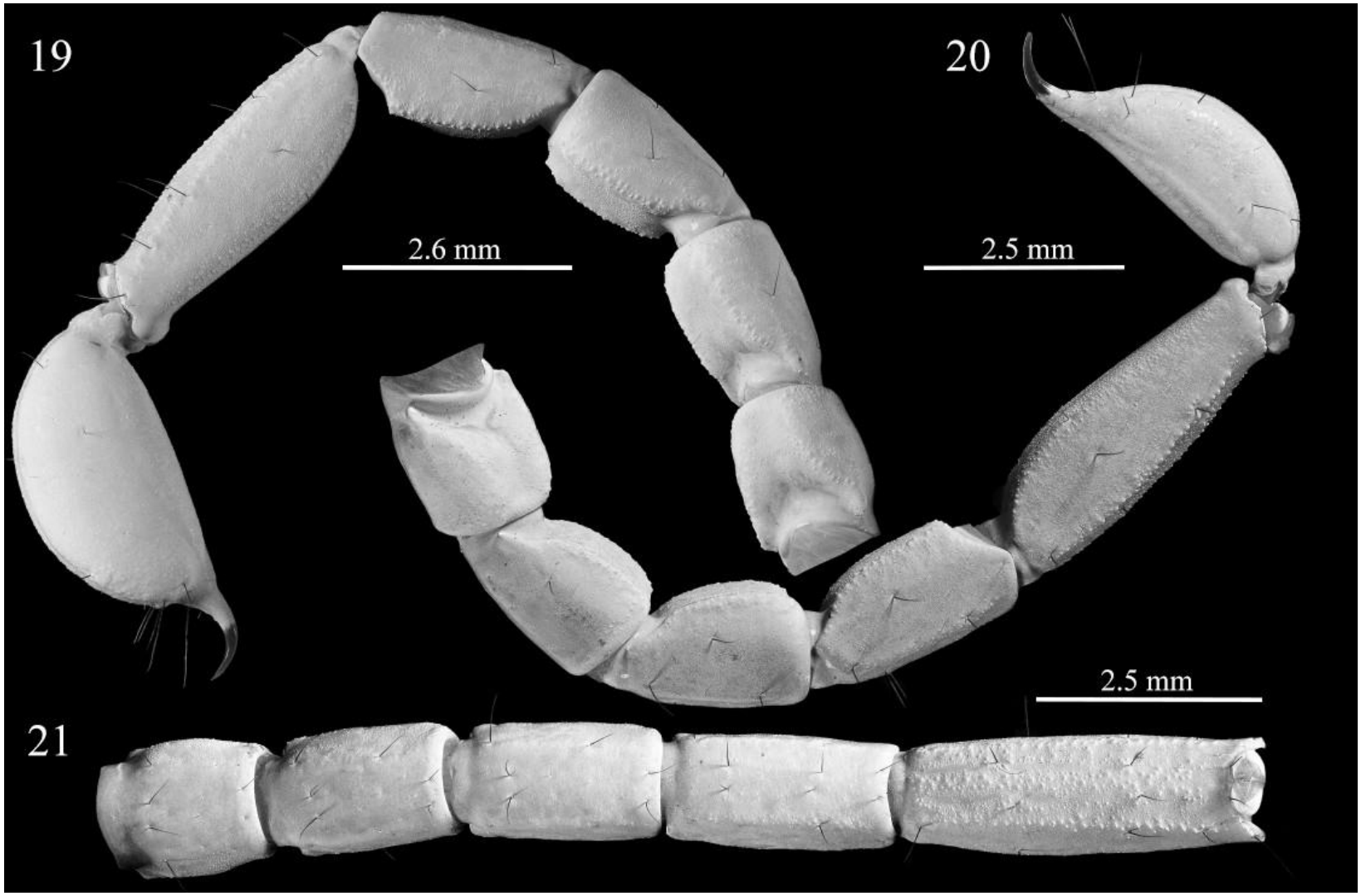

Plate 4. Figs. 19-21. *Euscorpius lagostae* Di Caporiacco, 1950: **Fig. 19.** Lateral aspect of metasoma segments I-V and telson, adult ♂ (VVZC2397). **Fig. 20.** Lateral aspect of metasoma segments I-V and telson, adult ♀ (VVZC1914). **Fig. 21.** Ventral aspect of metasoma segments I-V, adult ♀ (VVZC1914).

Lamelliform with elongated narrow sclerotized foot and trunk similar in length as flagellar lamina. Truncal flexure moderately developed. Capsule complex with one crown-like structure, basal lobe, distal internal and external lobe. Basal carina well developed with a small, sclerotized crown-like structure bearing 5 short straight spinules not equally distributed, but with one distant from the others which are closer together. Basal lobe elongated, with a distal straight margin and one small spine more basal (reduced, barely visible on right hemispermatophore). Distal internal lobe smooth, rounded shape, less sclerotized and smaller than distal external lobe. Distal external lobe large with rounded edge. Deep rounded basal constriction and laminar flagellar lamina with stronger sclerotized ventral margin and dorsal margin uniform without any hint of a notch.

Variability

The studied series (22 specimens) includes 10 adults, 2 subadults and 10 juveniles (2 are first-second instars). Intraspecific variation has been observed (first-second instars excluded except for trichobothria count) in the following aspects:

Coloration: Subadults have a similar coloration as adults while juveniles are overall lighter in color, pale yellowish; especially the pedipalp chela is lighter in color than adults. Only one juvenile specimen (VVZC2403) presents darker tergites (Fig. 8). Variability was observed on the coloration of the metasoma segments on all ontogenetic stages which can be darker due to the presence of marbling which varies from weak to moderate but always increasing in intensity from proximal to distal segments.

Marbling. Always very weak marbling and present on 10 adults as following: chelicera, only on dorsal distal surface (7/10), on entire dorsal surface (3/10); pedipalp chela (3/10); carapace (3/10); legs patella II-IV (1/10); metasomal segments (all specimens): I-V (7/20), II-V (10/20), III-V (1/20), IV-V (2/20).

Trichobothria. Pedipalp patella external counts (L/R): *eb*= 4/5 (1/22), 5/4 (1/22), 5/5 (20/22); eb_a= 6/6 (1/22), 7/7 (1/22), 7/8 (1/22), 8/7 (3/22), 8/8 (15/22), 8/9 (1/22); *esb*= 2/2 (22/22); *em*= 5/4 (1/22), 5/5 (21/22); *est*= 3/4 (1/22), 4/4 (21/22); *et*= 7/8 (1/22), 8/8 (8/22), 8/9 (1/22), 9/8 (3/22), 9/9 (9/22). Pedipalp patella ventral counts (L/R): 12/12 (12/22), 13/11 (1/22), 13/12 (3/22), 13/13 (5/22), 14/14 (1/22). Trichobothria *est-dsb* distance on adults show small variability without sexual correlation and all values (*et-est*/*est-dsb*) are between 0.77-1.14: 0.77 (1/10), 0.8 (1/10), 0.87 (1/10), 0.88 (1/10), 1 (5/10), 1.14 (1/10).

Pectines. Pectinal tooth count specimens (L/R): ♂♂: 8/9 (1/11), 9/8 (1/11), 9/9 (5/11), 9/10 (1/11), 10/8 (1/11) 10/9 (1/11), 10/10 (1/11); ♀♀: 6/3 (1/9), 8/8 (5/9), 8/9 (1/9), 9/8 (2/9). Middle lamellae count considering only the clearly separated lamellae is as following: ♂♂: 4/5 (1/10), 5/4 (1/10), 4/6 (1/10), 5/5 (4/10), 6/5 (1/10), 6/6 (2/10); ♀♀: 4/4 (1/10), 4/5 (2/10), 5/5 (1/10), 5/0 damaged pectine (1/10), 5/6 (2/10), 6/5 (2/10), 6/6 (1/10).

Morphosculpture. Punctuation of 10 adults is present on metasoma ventral surface of segment I (7/10) or absent (3/10); on tergites I-VII proximal portion and central-lateral portions punctuated and shagreened on central portions (5/10), proximal portion (2/10) or absent (3/10).

Telotarsi spinules. vary in number (10 adults): 8-13 on legs I-II-III, 7-13 on leg IV.

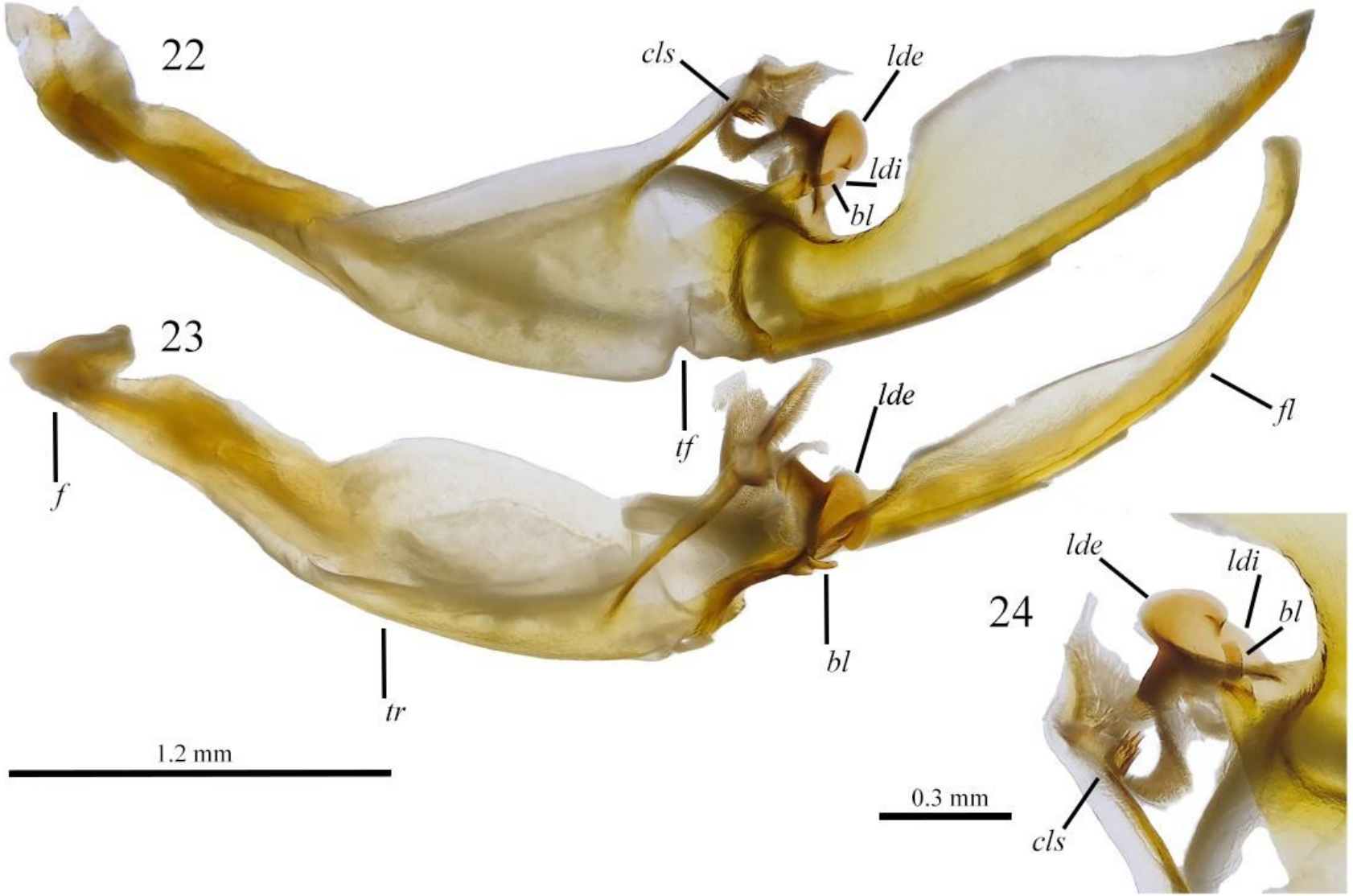

Plate 5. Figs. 22-24. *Euscorpius lagostae* Di Caporiacco, 1950: sinistral hemispermatophore (VVZC2398) **Fig. 22.** Ectal aspect. **Fig. 23.** Dorsal aspect**. Fig. 24.** Detail of capsular region. Abbreviations: foot: *f*; trunk: *tr*; truncal flexure: *tf*; flagellar lamina: *fl*; crown-like structure: *cls*; basal lobe: *bl*; distal external lobe: *lde*, distal internal lobe: *ldi*.

Fig. 25. *Euscorpius lagostae* Di Caporiacco, 1950, live habitus of adult ♀ (VVZC1914).

Ecology: habitats and sympatric scorpions

Our first two specimens were found on southern exposed part of Lastovo Island in June 2019. First discovery was close to the seashore in Uska bay near Skrivena Luka under stone in dry steno Mediterranean garrigue of *Erica multiflora* (leg. N. Tvrtković), while the second was observed in a sinkhole at the entrance of Rača cave, under stone in *Quercus ilex* coppice (leg. Marijana Vuković). In 2023 biospeleologist Tonći Rađa collected near one vertical cave in Zastražišće the first *E. lagostae* specimen from island Hvar, but without coordinates. This unexpected found motivate in September 2024 a 4-day field research expedition in Southern Croatia with the specific goal of collecting more specimens to deepen the morphological study, but also to observe the ecology and distribution of *E. lagostae*. A total of twelve sites has been investigated in two geographic areas, Pelješac Peninsula, and Hvar Island (Split-Dalmatia County). On the western part of Pelješac Peninsula the species was observed into two localities of four investigated. All were found under stones both in *Quercus ilex and Fraxinus ornus* wood (Donja Banda mine, Potomje) and mature mediterranean scrub, close to a stony wall near road before Nakovana (Figs. 26-27). In the latter locality the species was found in syntopy with a smaller *Euscorpius* species from *E. tergestinus* group (study in progress). Seven sites on the island of Hvar were studied, from East to West, near (or within) the following towns: Gdinj, Zastražišće, Humac, Stari Grad, Dol, Dol -Sv. Nikola peak and Velo Grabje; and the species was found only at two of the investigated locations (Dol, Dol-Sv. Nikola peak). Close to Dol town the species was observed in the adjacent *Pinus halepensis* tree forest with bushes of *Quercus ilex* community, in a small wood with limestone stony walls at the entrance of the town and inside the stony wall near Sv. Mihovila church. During the day they were found under *Pinus halepensis*

bark, while during night they were observed inside the wall crevices or errant on the ground and on trees. In one of these three localities (entrance of Dol town from Stari Grad side), *E. lagostae* was found syntopic with the same smaller *Euscorpius* species currently under investigation found at Nakovana in the Pelješac Peninsula. Even if we explored different habitats on Pelješac Peninsula and Hvar Island, the species was not found neither in meadows, garrigues, low mediterranean scrubs and close to the seashore. Additionally, we investigated a locality near Pelješac connection with mainland at the ruins of the Smrdan Grad castle at Klek, located near Opuzen on left bank of Neretva Rivera. Here a second instar specimen and one pedipalp chela of an adult *Euscorpius* sp. (*E. hadzii* complex) specimen were found. Even if the sampling was performed during the night, no other specimens were observed. Probably due to the elevated and open position of the castle and the presence of a strong cold wind represent the cause of not finding more specimens.

Figs. 26-27. *Euscorpius lagostae* Di Caporiacco, 1950 habitat in Nakovana (Nakovanj), Pelješac peninsula (Croatia).

The *E. lagostae* specimens seem to be very localized and habitat selective. *E. lagostae* can be considered probably a thermophilic species after previous findings on Lastovo (Uska bay) under dry limestone stones, however our results give evidence that it prefers less sunny exposed areas unlike some other *Euscorpius* species and has rarely been observed in dry open areas, never in pastures and dry *Pinus halepensis* forests. It was collected mostly into dense vegetation areas or limestone walls protected from direct sun by vegetation. The assumption to consider this species as habitat selective is supported by the finding of other *Euscorpius* species (publication in progress) into dryer Mediterranean habitats. Into the three localities where *E. lagostae* was found in sympatry with another species, *E. lagostae* appears to be dominant on the smaller species by occupying the stony walls covered by vegetation, while the other species were observed on the nearby sun exposed habitats under stones in two of the three localities. Only into the third locality, *E. lagostae* was observed during the night together with another smaller euscorpiid in a wooded and shady area. Since we rarely (only once but close to the seashore) observed *E. lagostae* under stones in a sun exposed habitat where instead the other species were observed, we assume this finding is not evidence of syntopy, but they were probably passing through because they were active during the observation and not stable in the area.

DISCUSSION

Phylogeography

Expanded sampling in this study confirmed pronounced phylogeographic structuring within the *Euscorpius hadzii* complex (PODNAR *et al*., 2021), revealed additional lineages (Klek, Višegrad, Figs. 2a, 3) and sublineages (Island Mljet, Figs. 2a, 3), as well as further phylogeographic subdivision within previously established lineages (groups Eh1a and Eh1b, Fig. 3). Divergence of the Eh1 and Eh2 groups was estimated in Pliocene at 4.93 Ma (95% HPD: 7.53-3.13 Ma), with diversification within both groups occurring mostly during the Pleistocene (Fig. 2b). PODNAR *et al*. (2021) applied two alternative calibration schemes: Calibration II, based solely on the *16S* substitution rate, which placed this divergence at 2.9 Ma (95% HPD: 4.7 - 1.5 Ma), and Calibration I, employing both *16S* and *COI* mutational rates, which yielded an older estimate of 4.4 Ma (95% HPD: 6.9 - 2.8 Ma). The present analysis was conducted under the same calibration framework (Calibration I). Notably, the 95% HPD interval of our estimate overlaps with the timeframe of the Messinian Salinity Crisis (5.96-5.33 Ma), a period marked by profound palaeoenvironmental transformations across the circum-Mediterranean region at the end of the Miocene (ROVERI *et al*., 2014), indicating temporal compatibility between the initial divergence within the *Euscorpius hadzii* complex and these Messinian environmental changes. During the Pleistocene, pronounced fine-scale phylogeographic structuring became established within the complex. On Mljet Island, the occurrence of three genetically distinct haplotypes separated by up to 1.8% *COI* divergence within a restricted geographic area is consistent with long-term paleo persistence of populations, as is the presence of highly divergent haplotypes on Lastovo island (Fig. 3). The observed phylogeographic pattern indicates the presence of at least eight microrefugia within the Croatian part of the study area, including Lastovo Island, Hvar and the western part of the Pelješac Peninsula, which harbours *Euscorpius lagostae*, and five additional geographically distinct microrefugial areas (Mljet Island, Lokrum Islet, Konavle, Dubrovnik coast and the mainland-proximal part of the Pelješac Peninsula) characterized by deeply divergent genetic lineages of yet unresolved taxonomic status (Figs. 2-3).

A comparable phylogeographic framework has been described for the sharp-snouted rock lizard *Dalmatolacerta oxycephala* (PODNAR *et al*., 2014), when considering populations assigned to the "Island clade" which encompassed much of the same geographic range as in the present study (including Lastovo Island, Mljet Island, Hvar Island and the Dubrovnik coast). Notably, *D. oxycephala* also comprises two major phylogeographic lineages, an Island and a Mainland clade, whose divergence was estimated at approximately 4.8 Ma (95% HPD: 7-3 Ma), temporally comparable to the divergence between the Eh1 and Eh2 groups in the *Euscorpius hadzii* complex. Thus, deep lineage splitting in both taxa occurred within a broadly similar late Miocene-early Pliocene timeframe. However, despite this temporal similarity, the phylogeographic pattern observed in the Eh1 group of the *Euscorpius lagostae* is characterized by deep phylogenetic structure (Eh1a and Eh1b; Figs. 2, 3) and highly divergent, spatially restricted haplotypes (Fig. 3). This pattern differs substantially from the one inferred for Island clade populations of *D. oxycephala* which belong to a single lineage and exhibit minimal haplotypic divergence across distant localities. The latter pattern was interpreted as the result of unintentional anthropogenic colonization, most plausibly via historical stone trade, the scenario

that could in principle also be invoked for scorpions. However, although human-mediated dispersal in Holocene via trade has been documented for euscorpiids (i.e. SCHEUCH *et al.*, 2020), the deep split between the Eh1a and Eh1b lineages (2.23 Ma; 95% HPD: 3.48-1.34), together with the presence of highly divergent and geographically structured haplotypes (Fig. 3), argues against the recent anthropogenic colonization or rapid postglacial radiation from a restricted source area and is instead more consistent with long-term in situ persistence in multiple microrefugia.

The discovery of new lineages - (i) two distinct lineages from the vicinity of Višegrad (Bosnia and Herzegovina, SCBIH53 and SCBIH66 in Fig. 2) located within the well-known NE Dinaric refugium harboring the European paleoendemic spruce *Picea omorika* (Pančić) Purk (HORVAT *et al*., 1974; ŠILIĆ, 1990), and (ii) a lineage from the hinterland hill above Klek near the mouth of the Neretva River (Croatia, SCBIH52 in Fig. 2), may provide a deeper insight into the poorly understood Pliocene history of the *E. hadzii* complex following detailed molecular investigation. At present, our results allow us to infer only that ancestral taxa of this complex were distributed during the Early Pliocene from the southeastern Croatian and Montenegrin coast, extending well into the Eastern Dinaric Alps. Potential Pliocene connections between the Eh2 lineage and *E. salentinus* Tropea, 2017 from Salento (southern Puglia, Italy) require further evaluation (Fig. 2a, Fig. S1, Fig. 8 in PODNAR *et al.*, 2021). If confirmed, such biogeographic scenario would parallel the patterns described in cave crickets of genus *Troglophilus* (Orthoptera, Rhaphidophoridae) (ALLEGRUCCI *et al*., 2017).

Molecular species delimitation

Overall, species delimitation analyses support two alternative scenarios for the Croatian populations. Eh1b clade = *Euscorpius lagostae,* as well as single specimen from Klek (SCBIH52) are consistently supported as a separate species by all four delimitation methods. Under the most conservative mPTP delimitation, the Eh1a clade = *E.* aff. *lagostae* represent single species, whereas distance-based methods support the presence of up to five putative species. The latter scenario is consistent with genetic divergences within and between the Eh1a + Eh1b clades reaching up to 5.2%, values comparable to or exceeding interspecific distances reported between *E. solegladi* and *E. hadzii* (FET *et al*., 2014). However, an integrative taxonomic approach, including detailed morphological analyses of populations not yet examined morphologically despite being included in the molecular dataset, will be required to determine whether the Croatian populations represent a single widespread species or multiple distinct species.

Differences from other Eastern Adriatic and related *Euscorpius* species

Euscorpius lagostae can be easily distinguished from all known Croatian *Euscorpius* species by the diagnostic trichobothria numbers (Figs. 17-18) of external pedipalp patella (Pe, *et*= 9 (8-9), especially *eba*=8, *em*=5) and ventral pedipalp patella (Pv=12). *Euscorpius solegladi* from Greece and Bulgaria is characterized by an oligotrichous trichobothrial pattern with Pv=10-11 and Pe, *et*=7, *eba*=5, *em*=4. Concerning other sister species of the *E. hadzii* group from the Balkans, there is no published review of the diagnostic traits. Statistical data for trichobothria counts in FET & SOLEGLAD (2002) from several examined Balkan specimens (of *E. hadzii* s.l.) in Fig. 46 are a mix

of data from at least five different species including *E. lagostae* and *E. solegladi.* In addition to the distinguishing characters among the two polytrichous species given by FET & SOLEGLAD (2002) we noticed that the telson vesicle in adult males is more swollen in *E. hadzii* than in *E. lagostae*. According to the morphometrics provided by FET & SOLEGLAD (2002) of two males the ratio vesicle length/height is 1.64, while the same ratio of the three males analyzed into the present study, the ratio average is 1.87. *E. lagostae* is not a species with a particular marked granular morphosculpture, but the noteworthy feature is that there is no evident sexual dimorphism in the granularity (Figs. 9-10) which is instead common among Euscorpiinae, where among sexually mature and older specimens, males have a noticeable stronger granularity than females.

Habitats

On Vis, Hvar, Pelješac and Lastovo there is a mosaic of the Eumediterranen vegetation (optimal habitats for forests with evergreen oak *Quercus ilex* and *Fraxinus ornus*) and drier Stenomediterranean vegetation sensu TRINAJSTIĆ (1986) such as garrigues with several West Mediterranean shrubs including *Erica multiflora* L., *Coronilla valentina* L. and *Phyllyrea angustifolia* L. (TRINAJSTIĆ, 1977). Only Pelješac has at higher altitudes and in wet and colder poljes (fields), Submediterranean *Quercus pubescens* (var. *virgiliana*) forests with *Carpinus orientalis* and *Osrya carpinifolia*. Submediterranean forests are also present along the Dubrovnik coast and Konavle, while Eumediterranean vegetation occurs only near the coast and on coastal islands and islets, such as Lokrum (ILIJANIĆ & HEĆIMOVIĆ, 1989). In contrast, populations of the Eh2 group live mainly at higher altitudes and represent montane taxa.

ACKNOWLEDGEMENTS

Special thanks to Dejan Kulijer for his hospitality and Denis Lešić for support during our exploration of and around the Pelješac peninsula. We are grateful to Fabrizio Turrisi (MZUF) for allowing the analysis of the type specimens and to Giuliano Trezzi, Branko Jalžić, Josip Skejo, Marijana Vuković, Toni Rađa and Petar Šuklje for their assistance in collecting samples. We thank Giuseppe Manganelli and Andrea Benocci (Museo di Storia Naturale Accademia dei Fisiocritici di Siena), Pierluigi Tolu (Circolo Fotografico Stile, Siena), Paolo Magrini, Augusto Degiovanni and Andrea Petrioli for providing support and technical advice. The study was partially funded by Croatian Science Foundation (Grant HRZZ-IP-2016-06-9988) ("DNA barcoding of Croatian faunal biodiversity").

Received March 3, 2026

REFERENCES

ALLEGRUCCI, G., KETMAIER, V., DI RUSSO, C., RAMPINI, M., SBORDINI, V. & COBOLLI, M., 2017: Molecular phylogeography of *Troglophilus* cave crickets (Orthoptera, Rhaphidophoridae): A combination of vicariance and dispersal drove diversification in the East Mediterranean region. Journal of Zoological Systematics and Evolutionary Research **55**(4), 310-325.

BANDELT, HJ., FORSTER, P. & RŐHL, A., 1999: Median-joining networks for inferring intraspecific phylogenies. Molecular Biology and Evolution **16**(1), 37-48. https://doi.org/10.1093/oxfordjournals.molbev.a026036

BARTOLOZZI, L., VANNI, S. & MASCHERINI, S. W., 1987: Catalogo del Museo Zoologico "La Specola" (Sezione del Museo di Storia Naturale) dell'Università di Firenze. 5. Arachnida Scorpiones: tipi. Atti della Società Toscana dei naturalisti. Memorie B, **94**, 293-298.

BLASCO-ARÓSTEGUI, J. & PRENDINI, L., 2023: Glacial Relicts? A New Scorpion from Mount Olympus, Greece (Euscorpiidae: *Euscorpius*). American Museum Novitates **36**. 10.1206/4003.1.

CAIN, S., GEFEN, E. & PRENDINI, L., 2021: Systematic revision of the Sand scorpions, genus *Buthacus* Birula, 1908 (Buthidae C. L. Koch, 1837) of the Levant, with redescription of *Buthacus arenicola* (Simon, 1885) from Algeria and Tunisia. Bulletin of the American Museum of Natural History **350**, 134 pp.

COUNCIL OF SCIENCE EDITORS, 2006: Scientific style and format. The CSE manual for authors, editors, and publishers, 7th ed. Reston, Virginia: Council of Science Editors, xvi + 658 pp.

DARRIBA, D., TABOADA, G. L., DOALLO, R., & POSADA, D., 2012: jModelTest 2: More models, new heuristics and parallel computing. Nature Methods, **9**, 772. https://doi.org/10.1038/nmeth.2109

DI CAPORIACCO, L., 1950: Le specie e sottospecie del genere "*Euscorpius*" viventi in Italia ed in alcune zone confinanti. Memorie/Accademia nazionale dei Lincei (ser. 8), **2**, 159-230.

FET, V., & SOLEGLAD, M. E., 2002: Morphology analysis supports presence of more than one species in the *"Euscorpius carpathicus"* complex (Scorpiones: Euscorpiidae). Euscorpius **3**, 1-51.

FET, V., SISSOM, W. D., LOWE, G., & BRAUNWALDER, M. E. (Eds.), 2000: Catalog of the scorpions of the world. New York: The New York Entomological Society.

FET, V., GANTENBEIN B., SOLEGLAD M. E., VIGNOLI V., SALOMONE N., FET E. & SCHEMBRI P. J., 2003: New molecular and morphological data on the "*Euscorpius carpathicus*" species complex (Scorpiones, Euscorpiidae) from Italy, Malta and Greece justify the elevation of *E. c. sicanus* (C. L. Koch, 1837) to the species level. Revue Suisse de Zoologie **110**, 335–379. https://doi.org/10.5962/bhl.part.80189

FET, V., GRAHAM, M.W.R., WEBBER, M.M. & BLAGOEV, G., 2014: Two new species of *Euscorpius* (Scorpiones: Euscorpiidae) from Bulgaria, Serbia, and Greece. Zootaxa, **3894**(1), 83-105.

GANTENBEIN, B. & LARGIADÈR, C. R., 2002: *Mesobuthus gibbosus* (Scorpiones: Buthidae) on the island of Rhodes – hybridization between Ulysses' stowaways and native scorpions? Molecular Ecology **11**, 925–938. https://doi.org/10.1046/j.1365-294X.2002.01494.x

GONZÁLEZ-SANTILLIÁN, E. & PRENDINI, L., 2013: Redefinition and generic revision of the North American vaejovid scorpion subfamily Syntropinae Kraepelin, 1905, with descriptions of six new genera. Bulletin of the American Museum of Natural History, **382**, 1-71.

GRAHAM, M. R., WEBBER, M. M., BLAGOEV, G., IVANOVA, N. & FET, V., 2012: Molecular and morphological evidence supports the elevation of *Euscorpius germanus croaticus* di Caporiacco, 1950 (Scorpiones: Euscorpiidae) to *E. croaticus* stat. nov., a rare species from Croatia. Revista Ibérica de Aracnología, **21,** 41-50.

HALL, T. A., 1999: BioEdit: A user-friendly biological sequence alignment editor and analysis program for Windows 95/98/NT. Nucleic Acids Symposium Series, **41**, 95-98.

HASSANIN, A., 2006: Phylogeny of Arthropoda inferred from mitochondrial sequences: strategies for limiting the misleading effects of multiple changes in pattern and rates of substitution. Molecular Phylogenetics and Evolution **38**(1), 100–116. https://doi.org/10.1016/j.ympev.2005.09.012

HEBERT, P. D., CYWINSKA, A., BALL, S. L. & DEWAARD, J. R., 2003: Biological identifications through DNA barcodes. Proceedings of the Royal Society B (Biological Sciences), **270** (1512), 313-320.

HJELLE, J.T., 1990: Anatomy and morphology, 9-63. In POLIS, G. A. (ed.), Biology of scorpions. Stanford, CA: Stanford University Press, 587 pp.

HORVAT, I., GLAVAČ, V. & ELLENBERG, H., 1974: Vegetation Südosteuropas. Geobotanica Selecta, Bd. 4, Gustav Fischer Verlag, Stuttgart, 768 pp.

HUELSENBECK, J. P., & RONQUIST, F., 2001: MRBAYES: Bayesian inference of phylogenetic trees. Bioinformatics, **17**, 754-755. https://doi.org/10.1093/bioin forma tics/17.8.754.

ICZN (International Commission on Zoological Nomenclature) 1999: International Code of Zoological Nomenclature. Fourth edition. International Trust for Zoological Nomenclature, London, 306 pp.

ILIJANIĆ, LJ. & HEĆIMOVIĆ, S., 1989: Vegetational and phytogeographical characteristics of the Dubrovnik area with special regard to the Island of Lokrum. 139 -163. In: MEŠIROV, M. & M. KEROVEC /eds./, Ekološke monografije 1, Hrvatsko ekološko društvo, Zagreb, 485 pp.

KAPLI, P., LUTTEROPP, S., ZHANG J., KOBERT, K., PAVLIDIS, P., STAMATAKIS, A. & FLOURI, T. 2017: Multi-rate Poisson tree processes for single-locus species delimitation under maximum likelihood and Markov chain Monte Carlo. Bioinformatics **33** (11), 1630–1638. https://doi.org/10.1093/bioinformatics/btx025

KOVAŘIK, F. & ŠT'ÁHLAVSKÝ, F., 2020: Five new species of *Euscorpius* Thorell, 1876 (Scorpiones: Euscorpiidae) from Albania, Greece, North Macedonia, and Serbia. Euscorpius, **315**, 1-37.

LACROIX, J. B., 1991a: Faune de France; Arachnida: Scorpionida. 5e note. Sub-genus (*Euscorpius*) Thorrel, 1876. Arachnides, **8**, 17-36.

LEIGH, J., W., & BRYANT, D., 2015: Popart: full-feature software for haplotype network construction. Methods in Ecology and Evolution **6**, 1110-1116. https://doi.org/10.1111/2041-210X.12410

LORIA, S. F. & PRENDINI, L., 2014: Homology of the Lateral Eyes of Scorpiones: A Six-Ocellus Model. PLoS ONE **9**. e112913. 10.1371/journal.pone.0112913.

MILLER, M., PFEIFFER, W. & SCHWARTZ, T., 2010: Creating the CIPRES Science Gateway for inference of large phylogenetic trees. In: Proceedings of the Gateway Computing Environments Workshop (GCE), 1-8. IEEE. https://doi.org/10.1109/GCE.2010.5676129

PARMAKELIS A., KOTSAKIOZI P., STATHI I., POULIKARAKOU S. & FET V. 2013: Hidden diversity of *Euscorpius* (Scorpiones: Euscorpiidae) in Greece revealed by multilocus species-delimitation approaches. Biological Journal of the Linnean Society **110**, 728–748. https://doi.org/10.1111/bij.12170

PODNAR, M., BRUVO MAĐARIĆ, B. & MAYER, W., 2014: Non-concordant phylogeographical patterns of three widely codistributed endemic Western Balkans lacertid lizards (Reptilia, Lacertidae) shaped by specific habitat requirements and different responses to Pleistocene climatic oscillations. Journal of Zoological Systematics and Evolutionary Research 52(2), 119–129. https://doi.org/10.1111/jzs.12056

PODNAR, M., GRBAC, I., TVRTKOVIĆ, N., HŐRWEG, C. & HARING, E., 2021: Hidden diversity, ancient divergences, and tentative Pleistocene microrefugia of European scorpions (Euscorpiidae: Euscorpiinae) in the eastern Adriatic region. Journal of Zoological Systematics and Evolutionary Research **59**(8), 1824 1849. https://doi.org/10.1111/jzs.12562

PUILLANDRE, N., LAMBERT, A., BROUILLET, S., & ACHAZ, G., 2012: ABGD, Automatic Barcode Gap Discovery for primary species delimitation. Molecular Ecology, **21**, 1864-1877. https://doi.org/10.1111/j.1365-294X.2011.05239.x

PUILLANDRE, N., BROUILLET, S., & ACHAZ, G., 2021: ASAP: Assemble Species by Automatic Partitioning. Molecular Ecology Resources, **21**, 609-620. https:// doi: 10.1111/1755-0998.13281.

RATNASINGHAM, S. & HEBERT, P. D. N., 2007: BOLD: The Barcode of Life Data System (http://www.barcodinglife.org). Molecular Ecology Notes **7**, 355-364.

RONQUIST, F., & HUELSENBECK, J. P., 2003: MRBAYES 3: Bayesian phylogenetic inference under mixed models. Bioinformatics, **19**, 1572-1574. https://doi.org/10.1093/bioinformatics/btg180

ROVERI, M., FLECKER, R., KRIJGSMAN, W., LOFI, J., LUGLI, S., MANZI, V., SIERRO, F. J., BERTINI, A., CAMERLENGHI, A., DE LANGE, G., GOVERS, R., HILGEN, F. J., HÜBSCHER, C., MEIJER, P. TH. & STOICA, M. 2014: The Messinian Salinity Crisis: Past and future of a great challenge for marine sciences. Marine Geology **352**, 25-58. https://doi.org/10.1016/j.margeo.2014.02.002

SALOMONE, N., VIGNOLI, V., FRATI, F. & BERNINI, F., 2007: Species boundaries and phylogeography of the "*Euscorpius carpathicus* complex" (Scorpiones: Euscorpiidae) in Italy. Molecular Phylogenetics and Evolution **43**, 502-514.

SCHEUCH, M., BALDRIAN, D., ELGHANDOUR, I., HARRAUER, E., HÖRWEG, C., LEINENBACH, L., PAUSER, I., SALZER, F., TRAPEL, L., VÖLKER, S. & WURZENBERGER, J., 2020: Der „Skorpion von Krems" - Status des nördlichsten Vorkommens von *Euscorpius tergestinus*. Biodiversität und Naturschutz in Ostösterreich -BCBEA **5**(1), 3-16.

SOLEGLAD, M. E. & SISSOM, W.D., 2001: Phylogeny of the family Euscorpiidae Laurie, 1896: a major revision. pp. 25 -112 in: FET, V. & SELDEN, P. A. (eds.), Scorpions 2001. In Memoriam Gary A. Polis. Burnham Beeches, Bucks, UK: British Arachnological Society.

SOLEGLAD, M. E. & FET, V., 2003: The scorpion sternum: structure and phylogeny (Scorpiones: Orthosterni). Euscorpius, **5**, 1-33. https://dx.doi.org/10.18590/euscorpius.2003.vol2003.iss5.1

STAHNKE, H. L., 1970: Scorpion nomenclature and mensuration. Entomological News, **81**, 297-316.

ŠTUNDLOVÁ J., ŠMÍD J., NGUYEN P. & ŠŤÁHLAVSKÝ F., 2019: Cryptic diversity and dynamic chromosome evolution in Alpine scorpions (Euscorpiidae: *Euscorpius*). Molecular Phylogenetics and Evolution **134**, 152-163. https://doi.org/10.1016/j.ympev.2019.02.002

ŠILIĆ, Č., 1990: Endemic plants. IP Svjetlost, Zavod za udžbenuke i nastavna sredstva, Sarajevo /Beograd, 227 pp.

TAMURA, K., STECHER, G. & KUMAR, S., 2021: MEGA11. Molecular Evolutionary Genetics Analysis Version 11. Molecular Biology and Evolution **38**(7), 3022-3027.

TRINAJSTIĆ, I., 1977: Grundzuge der Pflanzendecke der Inseln Hvar und ihre Pflanzengeographische Stellung im rahmen der Europaischen Teile des Mittelmeergebirge. (In Croatian with German Zusammenfassung). Poljoprivreda i šumarstvo, **23**(4), 1-33.

TRINAJSTIĆ, I., 1986: The phytogeographical division of the Eastern-Adriatic Mediterranean region -the starting point in the organization of managing the Mediterranean forests. (In Croatian with English Summary). Annales pro experementis, edition peculiaris, **2**, 53-67.

TROPEA, G., YAĞMUR, E. A. & YEŞILYURT, F., 2014: A new species of *Euscorpius* Thorell, 1876 from the Antalya Province, southern Turkey (Scorpiones: Euscorpiidae). Euscorpius, **184**, 1-13.

VACHON, M., 1974: Étude des caractèrés utílisés pour classer les familles et les genres de scorpions (Arachnides). 1. La trichobothriotaxie en arachnologie. Sigles trichobothriaux et types de trichobothriotaxie chez les scorpions. Bulletin du Muséum National d'Histoire naturelle, Paris, **140**, 859-958.

VENCES, M., MIRALLES, A., BROUILLET, S., DUCASSE, J., FEDOSOV, A., KHARCHEV, V., KUMARI, S., PATMANIDIS, S., PUILLANDRE, N., SCHERZ, M. D., KOSTANIDOV, I., & RENNER, S. S., 2021: iTaxoTools 0.1. Kickstarting a specimen-based software toolkit for taxonomists. Megataxa, **6**, 77-92. https://doi.org/10.11646/megataxa.6.2.1

VIGNOLI, V. & SALOMONE, N., 2008: A review of and additions to the current knowledge of the scorpion genus *Euscorpius* Thorell, 1876 (Scorpiones, Euscorpiidae), Fragmenta entomologica, **40**(2), pp. 189-228.

VOLSCHENK, E., S. 2005: A new technique for examining surface morphosculpture of scorpions. Journal of Arachnology, **33**, 820-825.

ZHANG J., KAPLI P., PAVLIDIS P., STAMATAKIS A., 2013: A general species delimitation method with applications to phylogenetic placements. Bioinformatics **29**(22), 2869-2876. https://doi.org/10.1093/bioinformatics/btt499

Supplement material:

Tab. S1. List of specimens included in the molecular analyses. Taxonomic designation, sample ID (DNA code), locality, BOLD accession numbers (mt*COI*) and the origin of the sequences are given. No. in the 4th column refers to the numbers shown on map (Fig. 1). Abbreviations: HR = Croatia, BG = Bulgaria, BIH = Bosnia and Herzegovina, MNE = Montenegro, AL = Albania.

Fig. S1. Bayesian phylogram based on the concatenated mitochondrial *COI* and *16S* sequences. Numbers at nodes indicate Bayesian posterior probabilities.